

Supporting Information

C-F bond activation of a perfluorinated ligand leading to nucleophilic fluorination of an organic electrophile.

Patrick J. Morgan,[§] Magnus W. D. Hanson-Heine,[§] Hayden P. Thomas,[†]
Graham C. Saunders,^{*,†} Andrew C. Marr,^{*,‡} Peter Licence.^{*,§}

[§]GSK Carbon Neutral Laboratory, School of Chemistry, University of Nottingham, NG7 2GA, United Kingdom

[‡]School of Chemistry and Chemical Engineering, Queen's University Belfast, David Keir Building, Belfast BT9 5AG, United Kingdom

[†]School of Science, University of Waikato, Hamilton 3240, New Zealand

Contents

1	Experimental details	S4
1.1	Instrumentation	S4
1.2	Materials	S4
1.3	Synthesis	S4
1.3.1	Synthesis of 2	S4
1.3.2	Synthesis of [Cp*RhCl ₂ (κC-MeNC ₃ H ₂ NCH ₂ C ₆ HF ₄)]	S5
1.3.3	Synthesis of [Cp*RhCl(κC ² -MeNC ₃ H ₂ NCH ₂ C ₆ F ₄)], 3	S5
1.3.4	ReactIR measurement of reaction of 1 with acetic anhydride	S6
1.3.5	UV photolysis of 1 with toluoyl chloride	S6
1.4	Fluorine transfer reactions	S7
1.4.1	General method for fluorine transfer between 1 and organic electrophiles.	S7
1.4.2	Acetic anhydride	S8
1.4.3	Benzoic anhydride	S8
1.4.4	Butyric anhydride	S8
1.4.5	Toluoyl chloride	S9

1.4.6 Benzoyl chloride.....	S9
1.4.7 4-nitrobenzoyl chloride.....	S9
1.4.8 Benzyl bromide.....	S10
1.4.9 2,3,4,5,6-pentafluorobenzyl bromide	S10
1.4.10 3-chloropenta-2,4-dione	S10
1.4.11 2-chloroacetaphenone	S11
1.5 Single crystal X-ray diffraction.	S12
1.6 DFT studies.....	S13
1.7 References	S14
2 Figures	S16
2.1 Figure S1. ¹ H NMR spectrum of 2	S16
2.2 Figure S2. ¹⁹ F NMR spectrum of 2	S17
2.3 Figure S3. ¹⁹ F NMR spectrum of reaction mixture with toluoyl fluoride and 2	S18
2.4 Figure S4. ¹⁹ F NMR spectrum of RhCp*Cl ₂ (F ₅ Bzmim) and 2 showing conversion.	S19
2.5 Figure S5. ¹ H NMR spectrum of [Cp*RhCl ₂ (κC-MeNC ₃ H ₂ NCH ₂ C ₆ HF ₄)].	S20
2.5 Figure S5. ¹⁹ F NMR spectrum of [Cp*RhCl ₂ (κC-MeNC ₃ H ₂ NCH ₂ C ₆ HF ₄)].	S21
2.7 Figure S7. ¹ H NMR spectrum of [Cp*RhCl(κC ² -MeNC ₃ H ₂ NCH ₂ C ₆ F ₄)], 3	S22
2.8 Figure S8. ¹⁹ F NMR spectrum of [Cp*RhCl(κC ² -MeNC ₃ H ₂ NCH ₂ C ₆ F ₄)], 3	S23
2.9 Figure S9. ¹⁹ F NMR spectrum of toluoyl fluoride following UV photolysis.	S24
2.10 Figure S10. ¹⁹ F NMR spectrum of sediment from cuvette following UV photolysis.	S25
2.11 Figure S11. Plot showing formation of toluoyl fluoride and consumption of 1 over time.	S26
2.12 Figure S12. ¹⁹ F NMR spectrum of acetyl fluoride.	S28
2.13 Figure S13. ¹⁹ F NMR spectrum of benzoyl fluoride.	S29
2.14 Figure S14. ¹⁹ F NMR spectrum of butyryl fluoride.	S30
2.15 Figure S15. ¹⁹ F NMR spectrum of toluoyl fluoride.....	S31
2.16 Figure S16. ¹⁹ F NMR spectrum of benzoyl fluoride.	S32
2.17 Figure S17. ¹⁹ F NMR spectrum of 4-nitrobenzoyl fluoride.	S33
2.18 Figure S18. ¹⁹ F NMR spectrum of benzyl fluoride.	S34
2.19 Figure S19. ¹⁹ F NMR spectrum of 2,3,4,5,6-pentafluorobenzyl fluoride.....	S35
2.20 Figure S20. ¹⁹ F NMR spectrum of 3-fluoropenta-2,4-dione.	S36
2.21 Figure S21. ¹⁹ F NMR spectrum of 2-fluoroacetaphenone.....	S37
2.22 Figure S22. Electrospray mass spectrum of 2	S38
2.23 Figure S23. Calculated ¹⁹ F NMR chemical shift of RhCp*Cl ₂ (F ₅ Bzmim).	S39
2.24 Figure S24. Calculated ¹⁹ F NMR chemical shift of 1	S40

1 Experimental details

1.1 Instrumentation

NMR spectral analysis was carried out using a Bruker Ascend 400 spectrometer (400 MHz) and Bruker Ascend 500 spectrometer (500 MHz) at room temperature (≈ 300 K). ^1H and ^{13}C NMR spectra were calibrated to the corresponding solvent signals (CDCl_3 : 7.26 ppm for ^1H , 77.16 ppm for ^{13}C). The ^{19}F NMR spectra were calibrated by an internal method of the NMR. The chemical shifts are reported in ppm and coupling constants are given in Hz. Electrospray mass spectra were recorded on a Bruker micrOTOF II with Agilent technologies 1200 Infinity Series mass spectrometer. *In-situ* ReactIR measurements conducted using Mettler Toledo ReactIR 15, collecting a spectral average of 256 scans at a scan rate of 256 scans per minute. Experiment set up and analysed using Mettler Toledo iC IR software. UV photolysis carried out using a high intensity mercury arc lamp, which was filtered using Pyrex and Newport FSQ-BG40 glass bandpass filter to limit irradiation of the sample by 308 and 360 nm wavelength. UV/Vis spectra were collected using an Agilent Cary 60 UV/Vis spectrophotometer, scanning from 800 nm to 200 nm at a scan rate of 600 nm/min. Glassware was oven-dried, evacuated and backfilled with argon before use.

1.2 Materials

$\text{RhCp}^*(\text{Cl}_2)(\text{F}_3\text{Bzmim})$ and **1** were synthesized as previously described.¹⁻³ 3-methyl-1-(3,4,5,6-tetrafluorobenzyl)-imidazolium bromide was synthesized using a similar procedure which has previously been described.¹ 1-methylimidazole, silver oxide, toluoyl chloride, benzoyl chloride, benzoic anhydride and butyric anhydride were purchased from Sigma Aldrich (Merck). $[\text{RhCp}^*\text{Cl}_2]_2$, 4-nitrobenzoyl chloride, benzyl bromide and 2-chloroacetophenone were purchased from Alfa Aesar. Acetic anhydride was purchased from VWR. 2,3,4,5,6-pentafluorobenzyl bromide and 3,4,5,6-tetrafluorobenzyl bromide were purchased from Fluorochem. 3-chloropenta-2,4-dione was purchased from Acros Organics. All solvents were purified, degassed and dried before use.

1.3 Synthesis

1.3.1 Synthesis of **2**.

Dichloromethane (5 mL) was added to a flask containing **1** (25 mg, 0.046 mmol). Once dissolved, toluoyl chloride (0.10 mmol, 2 equivalents) was added and the stirring continued for 1 week. The reaction mixture was removed from the glovebox, and the solvent removed *in vacuo* resulting in an orange crystalline powder and an orange oil. CDCl_3 (0.5 mL) was added and the solution transferred to a Young's valve NMR tube under argon. Analysis of the ^{19}F NMR showed up to 30 % conversion of **1** to **2**. Toluoyl fluoride was extracted with ether and **2** was recrystallized from a saturated solution of dichloromethane. Isolated yield: 3.5 mg (13.7 % yield)

¹H NMR (400 MHz, *d*₁-chloroform): δ 7.71 (d, *J*_{HH} = 3.3 Hz, HCCH, 1H), 7.70 (d, *J*_{HH} = 3.3 Hz, HCCH', 1H), 7.54 (d, *J*_{HH} = 3.3 Hz, HCCH, 1H), 7.53 (d, *J*_{HH} = 3.3 Hz, HCCH', 1H), 5.82 (d, *J*_{HH} = 16.5 Hz, CH₂, 2H), 5.56 (d, *J*_{HH} = 16.2 Hz, CH₂, 2H), 4.05 (s, CH₃, 6H), 1.87 (s, C₅-CH₂, 4H), 1.77 (s, C₅-CH₃, 6H), 1.40 (s, C₅-CH₃, 6H), 1.25 (s, C₅-CH₃, 6H), 0.92 (s, C₅-CH₃, 6H). **¹⁹F NMR** (376 Mhz, *d*₁-chloroform): δ -117.43 (s, C₆-F, 1F), -131.12 (d, *J*_{FF} = 19.9 Hz, C₆-F, 1F), -135.12 (d, *J*_{FF} = 20.9 Hz, C₆-F, 1F), -160.86 (t, *J*_{FF} = 22.8 Hz, C₆-F, 1F). **MS** (ESI) of **2**: Theoretical for C₂₁H₂₁Cl₁F₄N₂Rh [M/2-Cl]⁺ 515.0384; found [M/2-Cl]⁺ 515.0389. Theoretical for C₄₂H₄₂Cl₃F₈N₄Rh₂ [M-Cl]⁺ 1065.0457; found [M-Cl]⁺ 1065.0445. Satisfactory EA data could not be obtained, despite repeated attempts. Identity and purity have been established, to the best of our ability, using the aforementioned spectroscopic, crystallographic and MS data.

The formation of toluoyl fluoride was also identified: 1 mg (13.3 % yield; 97 % conversion vs 0.003 mmol of **2** formed {Figure S3})

¹H NMR (400 Mhz, *d*₁-chloroform): δ 7.99 (d, *J*_{HH} = 8.1 Hz, C₆-H, 2H), δ 7.27 (d, *J*_{HH} = 8.1 Hz, C₆-H, 2H), 2.43 (s, Me, 3H). **¹⁹F NMR** (376 Mhz, *d*₁-chloroform): δ 17.30 (s, 1F, COF). **MS** (ESI) of toluoyl fluoride: Theoretical [M-F]⁺ [C₈H₇O]⁺ 119.0497; found [C₈H₇O]⁺ 119.0498.

1.3.2 Synthesis of [Cp*RhCl₂(κC-MeNC₃H₂NCH₂C₆HF₄)].

Silver (I) oxide (0.041 g, 0.180 mmol) was added to a solution of 3-methyl-1-(3,4,5,6-tetrafluorobenzyl)-imidazolium bromide (0.088 g, 0.270 mmol) in dichloromethane (20 mL) under argon, in the absence of light. The mixture was stirred for 2 hours before filtration through a plug of celite and washed with dichloromethane (2 x 20 mL). [RhCp*RhCl₂]₂ (0.084 g, 0.135 mmol) was added to this solution, which was stirred for a further four hours under argon and in the absence of light. The crude reaction mixture was filtered through a plug of celite, washed with dichloromethane (2 x 20 mL) and the filtrate was concentrated under reduced pressure. The crude product was recrystallized from the concentrated solution of dichloromethane and pentane at -20 °C. Isolated yield: 0.127 g (85 %).

¹H NMR (400 MHz, *d*₁-chloroform): δ 7.56 (m, C₆-H, 1H), 7.03 (d, *J*_{HH} = 2.0 Hz, HCCH, 1H), 6.79 (d, *J*_{HH} = 2.0 Hz, HCCH, 1H), 6.40 (d, *J*_{HH} = 10.9 Hz, CH₂, 1H) 5.04 (d, *J*_{HH} = 13.6 Hz, CH₂, 1H), 4.03 (s, CH₃, 3H), 1.61 (s, C₅(CH₃)₅, 15H). **¹⁹F NMR** (376 MHz, *d*₁-chloroform): δ -137.31 (m, 1F), -145.46 (m, 1F), -155.06 (m, 1F), -156.07 (m, 1F). **¹³C NMR** (101 MHz, *d*₁-chloroform): δ 171.3 (d, *J*_{RhC} = 57 Hz, NCN), 147.3 (dd, *J*_{CF} = 249, 10 Hz, C-F), 145.8 (ddd, *J*_{CF} = 246, 3, 11 Hz, C-F), 140.4 (dm, *J*_{CF} = 255 Hz, C-F), 125.4 (HCCH), 122.2 (HCCH), 120.1 (m, C₆), 113.3 (m, C₆), 96.6 (d, *J*_{RhC} = 7 Hz, C₅), 45.8 (CH₂), 39.4 (CH₃), 9.5 (C₅(CH₃)₅). **MS** (ESI): Theoretical for C₂₁H₂₃F₄N₂ClRh [M - Cl]⁺ 517.0535; found [M - Cl]⁺ 517.0538.

1.3.3 Synthesis of [Cp*RhCl(κC²-MeNC₃H₂NCH₂C₆F₄)], **3**.

Silver (I) oxide (0.016 g, 0.07 mmol) added to a solution of [Cp*RhCl₂(κC-MeNC₃H₂NCH₂C₆HF₄)] (0.02 g, 0.035 mmol) in chloroform (10 mL) and left to stand for 24 hours in darkness under argon. The

crude reaction mixture was filtered through a plug of celite, washed with dichloromethane (2 x 10 mL) and the filtrate was concentrated under reduced pressure. The crude product was recrystallized from the concentrated solution of dichloromethane and hexane at -20 °C. Isolated yield: 0.012 g (65 %)

¹H NMR (*d*₁-chloroform): δ 7.08 (d, *J*_{HH} = 1.9 Hz, HCCH, 1H), 7.00 (d, *J*_{HH} = 1.9 Hz, HCCH, 1H), 5.27 (d, *J*_{HH} = 14.8 Hz, CH₂, 1H), 4.59 (d, *J*_{HH} = 14.8 Hz, CH₂, 1H), 3.96 (s, CH₃, 3H), 1.67 (s, Cp*, 15H). **¹⁹F NMR**: δ -110.35 (dd, *J*_{FF} = 14.0, 31.4 Hz, C₆-F, 1F), -146.83 (dd, *J*_{FF} = 14.2, 20.8 Hz, C₆-F, 1F), -157.99 (dd, *J*_{FF} = 19.5, 31.2 Hz, C₆-F, 1F), -164.44 (t, *J*_{FF} = 20.2 Hz, C₆-F, 1F). **Analysis** calcd. for C₂₁H₂₂ClF₄RhN₂·CHCl₃: C, 41.54; H, 3.64; N, 4.40 %. Found: C, 41.73; H, 3.89; N, 4.67 %. **MS** (ESI) of **3**: Theoretical for C₂₁H₂₂F₄N₂Rh [M-Cl]⁺ 481.0774; found [M-Cl]⁺ 481.0856.

1.3.4 ReactIR measurement of reaction of **1** with acetic anhydride

Dry, degassed ACN (5 mL) was added to a Schlenk flask under argon. The IR probe was inserted under a positive pressure of argon and a background taken using Mettler Toledo iC IR software. The IR probe was lowered into the ACN and the experiment started. **1** (20 mg, 0.037 mmol) was added after five minutes, followed by acetic anhydride (35 μL, 0.37 mmol) after a further 20 minutes, once the IR signal of **1** plateaued. Changes that occurred were monitored over time *via* the “solvent abstraction” feature of the iC IR software showed a clear reduction in signal intensity at 1386 cm⁻¹ (corresponding to **1**) and an increase in signal intensity at 1346 cm⁻¹ (corresponding to acyl fluoride), which became apparent at the 40 minute mark of the experiment. The reaction was monitored for 1 hour 30 minutes.

1.3.5 UV photolysis of **1** with toluoyl chloride

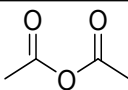
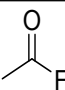
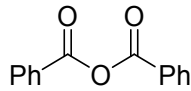
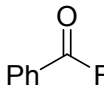
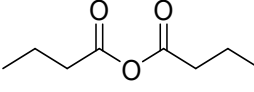
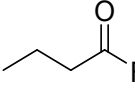
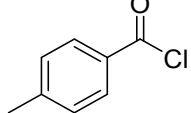
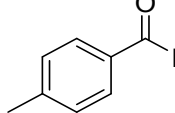
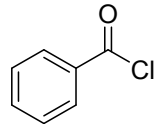
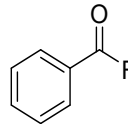
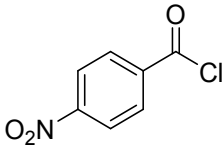
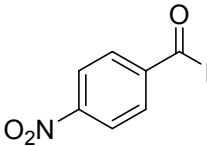
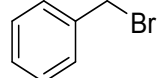
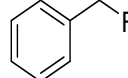
Toluoyl chloride (40 μL, 0.30 mmol) added to a solution of **1** (27 mg, 0.05 mmol) in dry, degassed deuterated ACN (5 mL) in an inert quartz reaction flask, fitted with a cuvette side arm (1 cm path length) under argon. The solution was transferred to the cuvette side arm, which was placed 5 cm in-front of a high intensity UV source from a mercury arc lamp. UV/Vis analysis was carried out by sampling the reaction mixture (0.1 mL reaction mixture made up to 10 mL with ACN in volumetric flask) over time, under argon. During the course of the reaction an orange sediment formed on the walls of the cuvette facing the UV source, which was found to be **2** following ¹⁹F NMR analysis and ESI-MS. The reaction mixture (0.5 mL) was transferred to Young’s tap NMR tube under argon, with α,α,α-trifluorotoluene (2 μL) for NMR analysis after 30 minutes. ¹⁹F NMR yield of toluoyl fluoride *vs* α,α,α-trifluorotoluene: 40 % yield.

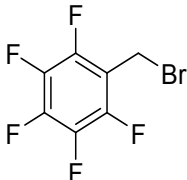
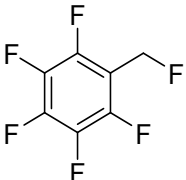
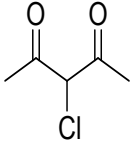
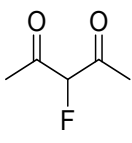
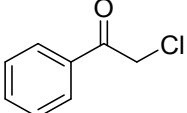
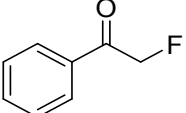
1.4 Fluorine transfer reactions

1.4.1 General method for fluorine transfer between **1** and organic electrophiles.

The organic electrophile (0.056 mmol) was added to a Young's tap NMR tube containing **1** (3 mg, 0.0056 mmol) and dry, degassed CD₃CN (0.5 mL), with α,α,α -trifluorotoluene (1 μ L) under argon. The contents of the tube were shaken and the reaction was monitored *via* ¹⁹F NMR over time. The conversion and formation of the fluorinated product are highlighted in Table S1, the substrate specific experimental is given below (Section 1.4.2 – 1.4.11). Due to the 10 equivalents of substrate added ¹H NMR analysis of products proved difficult in some cases due to overlapping signals. Products have been assigned using ¹⁹F NMR, referenced against literature precedent, where available. For some of the entries the difference between the observed yield of the fluorinated product and the conversion of **2** was due to the formation of a side-product, fluoroform. The difference observed was found to be comparable to the quantity of fluoroform formed, calculated against the internal standard.

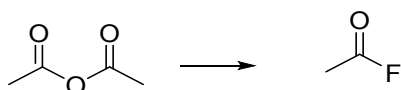
Table S1. Summary of the transfer fluorination reaction scope including substrate, product, time and ¹⁹F NMR conversion.

Entry	Substrate	Product	<i>t</i>	¹⁹ F NMR yield of fluorinated product [%] ^a	Conversion of organometallic [%] ^a
1			10 min	11.2	12.5
2			30 min	47.7	49.7
3			20 h	28.3	28.5
4			72 h	18.0	20.8
5			72 h	15.9	16.1
6			1 week	7.7	ND
7 ^b			1 week	7.5	11.6

8			1 week	9.9	12.5
9			1 week	trace	ND
10 ^b			1 week	trace	4.2

^a Determined by ¹⁹F NMR spectroscopy using α,α,α -trifluorotoluene as internal standard. ^b Fluorobenzene used as internal standard. ND – not determined.

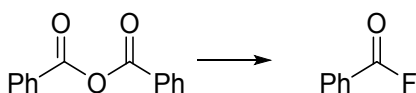
1.4.2 Acetic anhydride



The acetyl fluoride product was formed using the general method (Section 1.4.1). Acetic anhydride (6 mg, 0.056 mmol) was added to a Young's tap NMR tube containing **1** (3 mg, 0.0056 mmol) in dry, degassed CD₃CN (0.5 mL), with α,α,α -trifluorotoluene (1 μ L) under argon. The contents of the tube were shaken and the reaction monitored *via* ¹⁹F NMR over time. ¹⁹F NMR yield *vs.* the internal standard after 10 minutes: 11.2 %.

¹⁹F NMR (376 MHz, *d*₃-ACN): δ 48.91 (q, J_{HF} = 7.3 Hz, COF, 1F).⁴

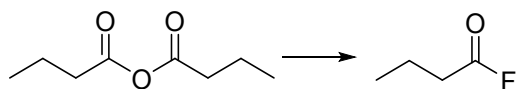
1.4.3 Benzoic anhydride



The benzoyl product was formed using the general method (Section 1.4.1). Benzoic anhydride (13 mg, 0.056 mmol) was added to a Young's tap NMR tube containing **1** (3 mg, 0.0056 mmol) in dry, degassed CD₃CN (0.5 mL), with α,α,α -trifluorotoluene (1 μ L) under argon. The contents of the tube were shaken and the reaction monitored *via* ¹⁹F NMR over time. ¹⁹F NMR yield *vs.* the internal standard after 30 minutes: 47.7 %.

¹H NMR (400 Mhz, *d*₃-ACN): δ 8.01 (d, J_{HH} = 7.5 Hz, C₆-H, 2H), δ 7.56 (t, J_{HH} = 8.1 Hz, C₆-H, 1H), 7.46 (t, J_{HH} = 7.7 Hz, C₆-H, 2H). ¹⁹F NMR (376 MHz, *d*₃-ACN): δ 16.57 (s, COF, 1F).⁵

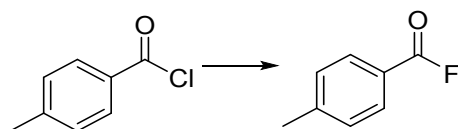
1.4.4 Butyric anhydride



The butanoyl fluoride product was formed using the general method (*Section 1.4.1*). Butyric anhydride (12 mg, 0.056 mmol) was added to a Young's tap NMR tube containing **1** (3 mg, 0.0056 mmol) in dry, degassed CD₃CN (0.5 mL), with α,α,α -trifluorotoluene (1 μ L) under argon. The contents of the tube were shaken and the reaction monitored *via* ¹⁹F NMR over time. ¹⁹F NMR yield *vs.* the internal standard after 20 hours: 28.3 %.

¹⁹F NMR (376 MHz, *d*₃-ACN): δ 43.10 (s, COF, 1F).⁴

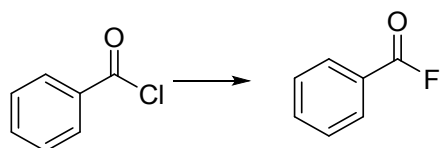
1.4.5 Toluoyl chloride



The toluoyl fluoride product was formed using the general method (*Section 1.4.1*). Toluoyl chloride (9 mg, 0.056 mmol) was added to a Young's tap NMR tube containing **1** (3 mg, 0.0056 mmol) in dry, degassed CD₃CN (0.5 mL), with α,α,α -trifluorotoluene (1 μ L) under argon. The contents of the tube were shaken and the reaction monitored *via* ¹⁹F NMR over time. ¹⁹F NMR yield *vs.* the internal standard after 72 hours: 18.0 %.

¹H NMR (400 Mhz, *d*₃-ACN): δ 7.92 (dt, J_{HH} = 1.9, 8.2 Hz, C₆-H, 2H), δ 7.33 – 7.30 (m, C₆-H, 2H), 2.42 (s, Me, 3H). ¹⁹F NMR (376 MHz, *d*₃-ACN): δ 15.85 (s, COF, 1F).⁶

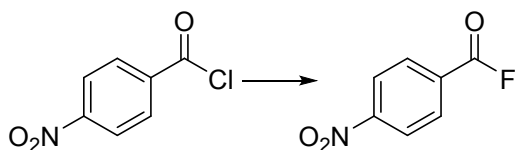
1.4.6 Benzoyl chloride



The benzoyl fluoride product was formed using the general method (*Section 1.4.1*). Benzoyl chloride (8 mg, 0.056 mmol) was added to a Young's tap NMR tube containing **1** (3 mg, 0.0056 mmol) in dry, degassed CD₃CN (0.5 mL), with α,α,α -trifluorotoluene (1 μ L) under argon. The contents of the tube were shaken and the reaction monitored *via* ¹⁹F NMR over time. ¹⁹F NMR yield *vs.* the internal standard after 72 hours: 15.9 %.

¹H NMR (400 Mhz, *d*₁-chloroform): δ 7.96 (d, J_{HH} = 7.5 Hz, C₆-H, 2H), δ 7.56 (t, J_{HH} = 8.1 Hz, C₆-H, 1H), 7.43 (t, J_{HH} = 7.7 Hz, C₆-H, 2H). ¹⁹F NMR (376 MHz, *d*₃-ACN): δ 16.55 (s, COF, 1F).⁵

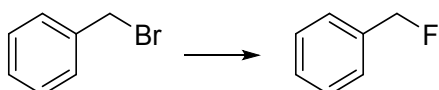
1.4.7 4-nitrobenzoyl chloride



The 4-nitrobenzoyl fluoride product was formed using the general method (*Section 1.4.1*). 4-nitrobenzoyl chloride (11 mg, 0.056 mmol) was added to a Young's tap NMR tube containing **1** (3 mg, 0.0056 mmol) in dry, degassed CD₃CN (0.5 mL), with α,α,α -trifluorotoluene (1 μ L) under argon. The contents of the tube were shaken and the reaction monitored *via* ¹⁹F NMR over time. ¹⁹F NMR yield *vs.* the internal standard after 1 week: 7.7 %.

¹⁹F NMR (376 MHz, *d*₃-ACN): δ 19.69 (s, COF, 1F).⁷

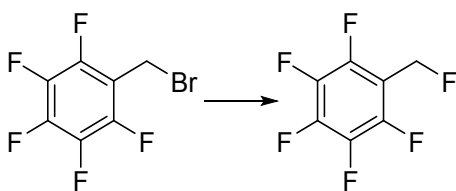
1.4.8 Benzyl bromide



The benzyl fluoride product was formed using the general method (*Section 1.4.1*). Benzyl bromide (10 mg, 0.056 mmol) was added to a Young's tap NMR tube containing **1** (3 mg, 0.0056 mmol) in dry, degassed CD₃CN (0.5 mL), with α,α,α -trifluorotoluene (1 μ L) under argon. The contents of the tube were shaken and the reaction monitored *via* ¹⁹F NMR over time. ¹⁹F NMR yield *vs.* the internal standard after 1 week: 7.5 %.

¹⁹F NMR (376 MHz, *d*₃-ACN): δ -205.91 ppm (t, J_{FF} = 48.2 Hz, 1F).⁸

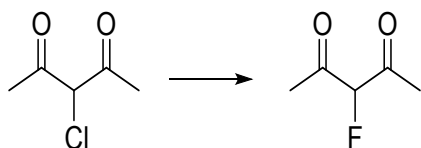
1.4.9 2,3,4,5,6-pentafluorobenzyl bromide



The 2,3,4,5,6-pentafluorobenzyl fluoride product was formed using the general method (*Section 1.4.1*). 2,3,4,5,6-pentafluorobenzyl bromide (15 mg, 0.056 mmol) was added to a Young's tap NMR tube containing **1** (3 mg, 0.0056 mmol) in dry, degassed CD₃CN (0.5 mL), with α,α,α -trifluorotoluene (1 μ L) under argon. The contents of the tube were shaken and the reaction monitored *via* ¹⁹F NMR over time. ¹⁹F NMR yield *vs.* the internal standard after 1 week: 9.9 %.

¹⁹F NMR (376 MHz, *d*₃-ACN): δ -211.79 (t, J_{HF} = 46 Hz, COF, 1F) -144.51 (dd, J_{FF} = 14.0, 31.4 Hz, C₃F₃C₂F₂C), -155.77 (dt, J_{FF} = 14.2, 20.8 Hz, C₅F₄CF), -163.93 (m, C₃F₂C₂F₂CF).⁹

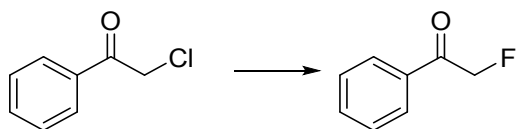
1.4.10 3-chloropenta-2,4-dione



The 3-fluoropenta-2,4-dione product was formed using the general method (Section 1.4.1). 3-chloropenta-2,4-dione (14 mg, 0.056 mmol) was added to a Young's tap NMR tube containing **1** (3 mg, 0.0056 mmol) in dry, degassed CD₃CN (0.5 mL), with α,α,α -trifluorotoluene (1 μ L) under argon. The contents of the tube were shaken and the reaction monitored *via* ¹⁹F NMR over time. ¹⁹F NMR yield *vs.* the internal standard after 1 week: trace.

¹⁹F NMR (376 MHz, *d*₃-ACN): δ -231.98 (s, COF, 1F).

1.4.11 2-chloroacetaphenone



The 2-fluoroacetaphenone product was formed using the general method (Section 1.4.1). 2-chloroacetaphenone (9 mg, 0.056 mmol) was added to a Young's tap NMR tube containing **1** (3 mg, 0.0056 mmol) in dry, degassed CD₃CN (0.5 mL), with α,α,α -trifluorotoluene (1 μ L) under argon. The contents of the tube were shaken and the reaction monitored *via* ¹⁹F NMR over time. ¹⁹F NMR yield *vs.* the internal standard after 1 week: trace.

¹⁹F NMR (376 MHz, *d*₃-ACN): δ -234.13 (t, J_{HF} = 45 Hz, COF, 1F).¹⁰

1.5 Single crystal X-ray diffraction.

Table S2. Crystal data and refinement for 2 and 3.

<i>Crystal Data</i>	2	[Cp*RhCl(κ C ² -MeNC ₃ H ₂ NCH ₂ C ₆ F ₄)], 3
CCDC number	1978328	1977788
Formula	C ₄₄ H ₄₆ Cl ₈ F ₈ N ₄ Rh ₂	C ₂₂ H ₄₃ Cl ₄ N ₂ Rh
Formula weight	1272.27	636.15
Temperature/K	120(2)	100(10)
Crystal system	monoclinic	monoclinic
Space group	P2 ₁ /n	P2 ₁ /n
<i>Unit cell dimensions</i>		
a	31.2523(17) Å	11.3192(11) Å
b	14.5067(3) Å	15.8568(4) Å
c	15.5905(8) Å	21.174(2) Å
α	90 °	90 °
β	136.763(10) °	139.96(2) °
γ	90 °	90 °
v	4841.9(7) Å ³	2444.7(11) Å ³
Z	4	4
ρ_{calc}	1.745 g/cm ³	1.7283 g/cm ³
μ	10.176 /mm ⁻¹	10.077 /mm ⁻¹
F	2544 (0 0 0)	1281.7 (0 0 0)
Crystal size	0.072 × 0.053 × 0.014 mm ³	0.147 × 0.076 × 0.041 mm ³
<i>Data collection and reduction</i>		
Diffractometre	SuperNova	SuperNova
Radiation	CuK α (λ = 1.54184)	CuK α (λ = 1.54184)
2 Θ (min - max)	5.98 to 148.814 °	8.56 to 147.82 °
Index ranges	-37 ≤ h ≤ 38, -17 ≤ k ≤ 17, -18 ≤ l ≤ 19	-13 ≤ h ≤ 13, -19 ≤ k ≤ 19, -26 ≤ l ≤ 25
Reflections collected	21420	22813
Independent reflections	9626 [R _{int} = 0.0259, R _{sigma} = 0.0327]	4874 [R _{int} = 0.0588, R _{sigma} = 0.0407]
Refinement method	Full-matrix least squares on F ²	Full-matrix least squares on F ²
Data/restraints/parameters	9626/0/605	4874/0/304
Goodness-of-fit on F ²	1.008	1.038
Final R indexes [I ≥ 2 σ (I)]	R ₁ = 0.0272, wR ₂ = 0.0651	R ₁ = 0.0417, wR ₂ = 0.1083
Final R indexes [all data]	R ₁ = 0.0341, wR ₂ = 0.0686	R ₁ = 0.0537, wR ₂ = 0.1200
Largest diff. peak/hole	0.90/-0.64 (e Å ⁻³)	0.97/-1.04 (e Å ⁻³)

1.6 DFT studies

Density functional theory (DFT) geometry optimizations, transition state searches, NMR shifts, energy and electron density calculations were performed with a developmental version of the Q-Chem software package.¹¹ Geometry optimization steps were carried out using the PBE0 exchange-correlation functional with the Los Alamos National Laboratory 2 double- ζ (LANL2DZ) pseudopotential and basis set used for the Rh atom and 6-31G(d) basis set for the lighter atoms.^{12,13} Geometries were confirmed as minima by the absence of imaginary harmonic vibrational frequencies present for these structures.

Energies and electron densities were then evaluated at these geometries using the 6-311++G(d,p) basis set for the light atoms and the Stuttgart Relativistic Small Core (SRSC) pseudopotential and basis set for rhodium.¹⁴ Interaction energies for the fluorine atoms were calculated from the difference between the complex energy and the sum of the isolated F atom and remaining fragment energies using the counterpoise correction method to account for basis set superposition error with all the associated fragment calculations performed using the same basis set as the complete complex.¹⁵ The interaction energies are given by:

$$E_{\text{int}} = - [E(\text{AB}) - E(\text{A}) - E(\text{B})] \quad 1$$

where $E(\text{AB})$ is the energy of the whole molecule, $E(\text{A})$ is the energy of the molecule with the fluorine atom removed and $E(\text{B})$ is the energy of the isolated fluorine atom, and natural population analysis (NPA) was then used to determine the charge on each fluorine atom.¹⁶

¹⁹F NMR chemical shifts were evaluated at the minima energy geometries using the gauge-invariant atomic orbital (GIAO) method with the B3LYP functional and a combination of the 6-31+G(d,p) basis for the atoms of the ring system, 6-31G(d,p) for all other non-metal atoms, and the all-electron 3-21G basis set for Rh.^{17,18} This level of theory was chosen to increase the applicability of established NMR scaling factors,¹⁹ while avoiding issues with linear dependence in the basis set and convergence during the GIAO NMR calculation. The scaled chemical shifts were calculated using the formula:

$$\sigma_{\text{scaled}} = \frac{\theta_{\text{isotropic}} - C}{M} \quad 2$$

where $\theta_{\text{isotropic}}$ is the unscaled isotropic chemical shift, while M and C are the gradient and the y-intercept of the fitting data, with values of -0.9652 and 194.71, respectively.

The DFT bond lengths calculated for the optimized geometry of **2** are within 0.077 Å of the experimental data (Table S3). The largest deviation occurs for the Rh – Cp* bond lengths where Rh2 – C4B has a difference of 0.077 Å. Rh1 – C4A has a bond length variation of 0.07. The calculated Rh2 – C5B bond length shows only a slight variation from the experimental result, with a difference of just 0.003 Å. There is a relatively large deviation in the calculated bond lengths of the C – F bonds, where the difference in the distance between C12A – F17A is 0.027 Å, while the C14A – F18A difference is 0.001 Å. The selected bond angles, given in Table S3, show very close agreement with the experiments results, and the largest deviation of 1.36° is seen between the Cp* centroid and the NHC carbon bound to the metal centre (C23B). Table S3 highlights selected bond lengths and angles for both the calculated and experimental data.

Table S3. Selected experimental and calculated bond lengths (Å) and bond angles (°) for 2.

Bond	Experimental	Calculated
Cp* – Rh ^a	1.8093(2)	1.8550
Rh1 – C26B	2.063(3)	2.036
Rh1 – Cl1	2.4129(6)	2.430
Rh1 – Cl2	2.4012(6)	2.414
C10A – C11A	1.518(3)	1.512
C11A – C12A	1.388(3)	1.390
C14A – C15A	1.387(4)	1.392
C12A – F17A	1.349(3)	1.333
C14A – F18A	1.345(3)	1.344
C15A – F19A	1.353(3)	1.328
C16A – F20A	1.341(3)	1.333
Cp* – Rh1 – C23B ^a	130.982(8)	132.34
Cp* – Rh1 – Cl2 ^a	120.930(5)	121.35
C1A – C10A – C11A	111.3(2)	113.23
C1B – C10B – C11B	113.3(2)	113.33
C12A – C11A – C16A	115.4(2)	115.61
C11A – C12A – C13A	125.5(2)	125.17
Cl1 – Rh1 – Cl2	86.6(2)	87.73
N22A – C21A – C13A	112.0(2)	112.26

^aCp* represents the centroid of the η⁵-pentamethylcyclopentadienyl ring

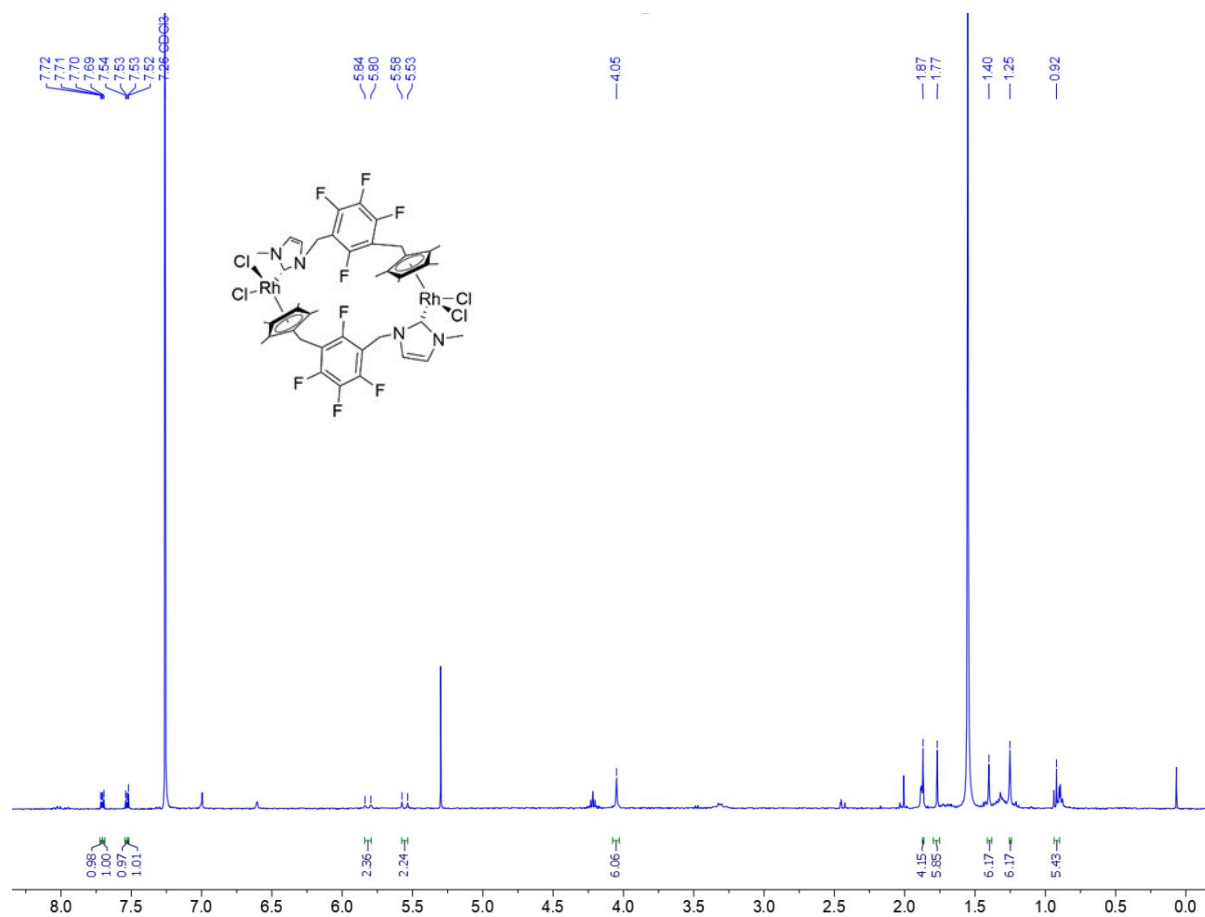
1.7 References

- (1) McGrandle, S.; Saunders, G. C. Group 9 Complexes of an N-Heterocycle Carbene Bearing a Pentafluorobenzyl Substituent: Attempted Dehydrofluorinative Coupling of Cyclopentadienyl and N-Heterocycle Carbene Ligands. *J. Fluor. Chem.* **2005**, *126*, 449–453.
- (2) Ma, Y.; Wang, Y.-M.; Morgan, P. J.; Jackson, R. E.; Liu, X.; Saunders, G. C.; Lorenzini, F.; Marr, A. C. Designing Effective Homogeneous Catalysis for Glycerol Valorisation: Selective Synthesis of a Value-Added Aldehyde from 1,3-Propanediol via Hydrogen Transfer Catalysed by a Highly Recyclable, Fluorinated Cp*Ir(NHC) Catalyst. *Catal. Today* **2018**, *307*, 248–259.
- (3) Thomas, H. P.; Marr, A. C.; Morgan, P. J.; Saunders, G. C. Tethering of Pentamethylcyclopentadienyl and N-Heterocycle Stabilized Carbene Ligands by Intramolecular 1,4-Addition to a Polyfluorophenyl Substituent. *Organometallics* **2018**, *37*, 1339–1341.
- (4) Dmowski, W.; Kamiński, M. Dialkyl- α,α -difluorobenzylamines and Dialkyl(trifluoromethyl)-Amines - Novel Fluorinating Reagents. *J. Fluor. Chem.* **1983**, *23*, 219–228.
- (5) Munoz, S. B.; Dang, H.; Ispizua-Rodriguez, X.; Mathew, T.; Prakash, G. K. S. Direct Access to Acyl Fluorides from Carboxylic Acids Using a Phosphine/Fluoride Deoxyfluorination Reagent System. *Org. Lett.* **2019**, *21*, 1659–1663.
- (6) Leclerc, M. C.; Bayne, J. M.; Lee, G. M.; Gorelsky, S. I.; Vasiliu, M.; Korobkov, I.; Harrison, D. J.; Dixon, D. A.; Baker, R. T. Perfluoroalkyl Cobalt(III) Fluoride and Bis(Perfluoroalkyl) Complexes: Catalytic Fluorination and Selective Difluorocarbene Formation. *J. Am. Chem. Soc.* **2015**, *137*, 16064–16073.
- (7) Scattolin, T.; Deckers, K.; Schoenebeck, F. Direct Synthesis of Acyl Fluorides from Carboxylic Acids with the Bench-Stable Solid Reagent (Me₄N)SCF₃. *Org. Lett.* **2017**, *19*, 5740–5743.
- (8) Xiang, M.; Xin, Z. K.; Chen, B.; Tung, C. H.; Wu, L. Z. Exploring the Reducing Ability of Organic Dye (Acr⁺-Mes) for Fluorination and Oxidation of Benzylic C(Sp³)-H Bonds under Visible Light Irradiation. *Org. Lett.* **2017**, *19*, 3009–3012.
- (9) Olah, G. A.; Comisarow, M. B. Stable Carbonium Ions. Alkyl(Aryl)Halocarbonium Ions and Haloarylcarbonium Ions. *J. Am. Chem. Soc.* **1969**, *91*, 2955–2961.
- (10) Wu, S. W.; Liu, F. Synthesis of α -Fluoroketones from Vinyl Azides and Mechanism Interrogation. *Org. Lett.* **2016**, *18*, 3642–3645.
- (11) Shao, Y.; Gan, Z.; Epifanovsky, E.; Gilbert, A. T. B.; Wormit, M.; Kussmann, J.; Lange, A. W.; Behn, A.; Deng, J.;

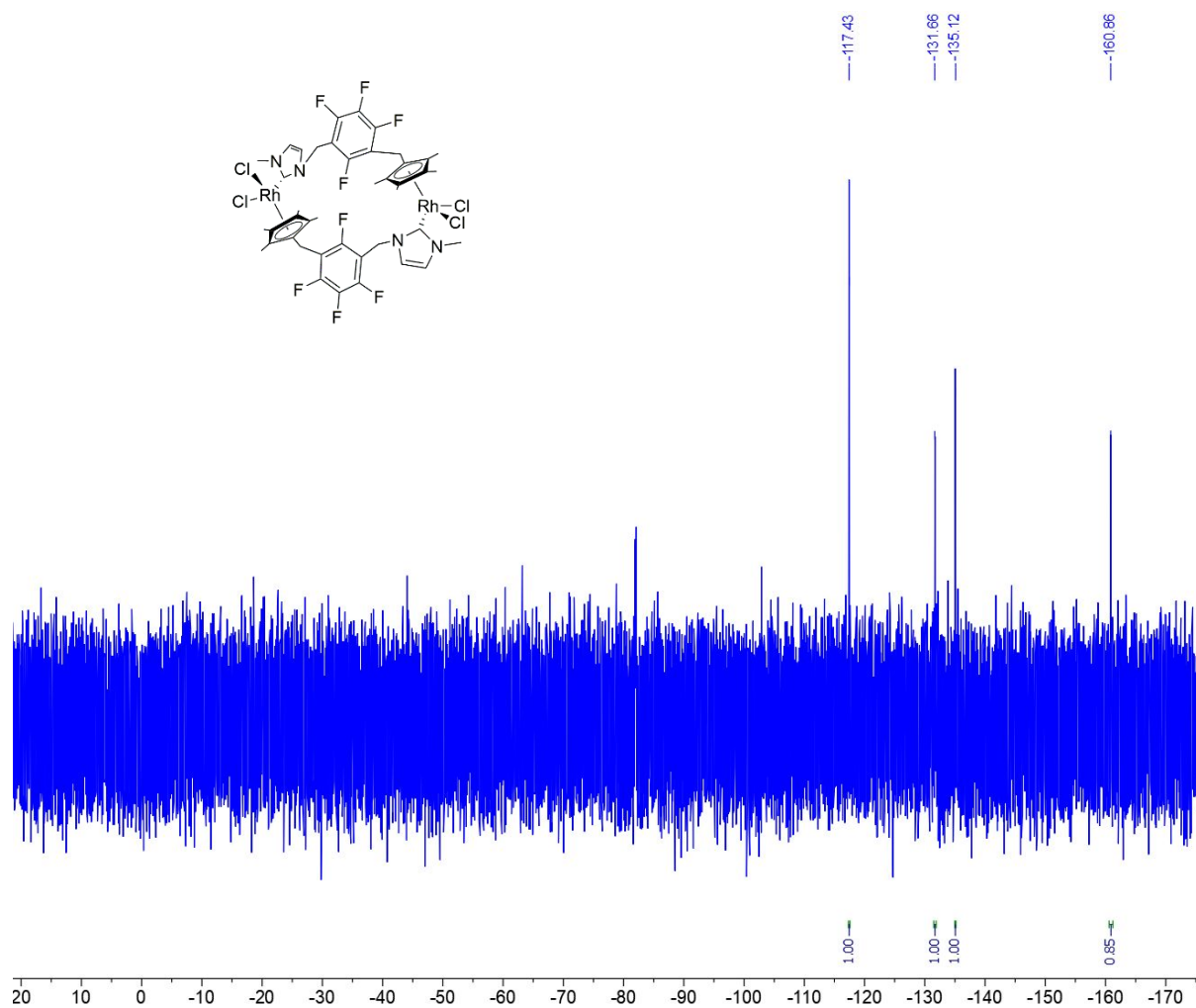
- Feng, X.; et al. Advances in Molecular Quantum Chemistry Contained in the Q-Chem 4 Program Package. *Mol. Phys.* **2015**, *113*, 184–215.
- (12) Hay, P. J.; Wadt, W. R. Ab Initio Effective Core Potentials for Molecular Calculations. Potentials for K to Au Including the Outermost Core Orbitals. *J. Chem. Phys.* **1985**, *82*, 299–310.
 - (13) Adamo, C.; Scuseria, G. E.; Barone, V. Accurate Excitation Energies from Time-Dependent Density Functional Theory: Assessing the PBE0 Model. *J. Chem. Phys.* **1999**, *111*, 2889–2899.
 - (14) Dolg, M.; Wedig, U.; Stoll, H.; Preuss, H. Energy-adjusted Ab Initio Pseudopotentials for the First Row Transition Elements. *J. Chem. Phys.* **1987**, *86*, 866–872.
 - (15) Boys, S. F.; Bernardi, F. The Calculation of Small Molecular Interactions by the Differences of Separate Total Energies. Some Procedures with Reduced Errors. *Mol. Phys.* **1970**, *19*, 553–566.
 - (16) Reed, A. E.; Curtiss, L. A.; Weinhold, F. Intermolecular Interactions from a Natural Bond Orbital, Donor—Acceptor Viewpoint. *Chem. Rev.* **1988**, *88*, 899–926.
 - (17) Becke, A. D. A New Mixing of Hartree-Fock and Local Density-Functional Theories. *J. Chem. Phys.* **1993**, *98*, 1372–1377.
 - (18) Bader, R. F. W. A Quantum Theory of Molecular Structure and Its Applications. *Chem. Rev.* **1991**, *91* (5), 893–928.
 - (19) Saunders, C.; Khaled, M. B.; Weaver, J. D.; Tantillo, D. J. Prediction of ¹⁹F NMR Chemical Shifts for Fluorinated Aromatic Compounds. *J. Org. Chem.* **2018**, *83*, 3220–3225.

2 Figures

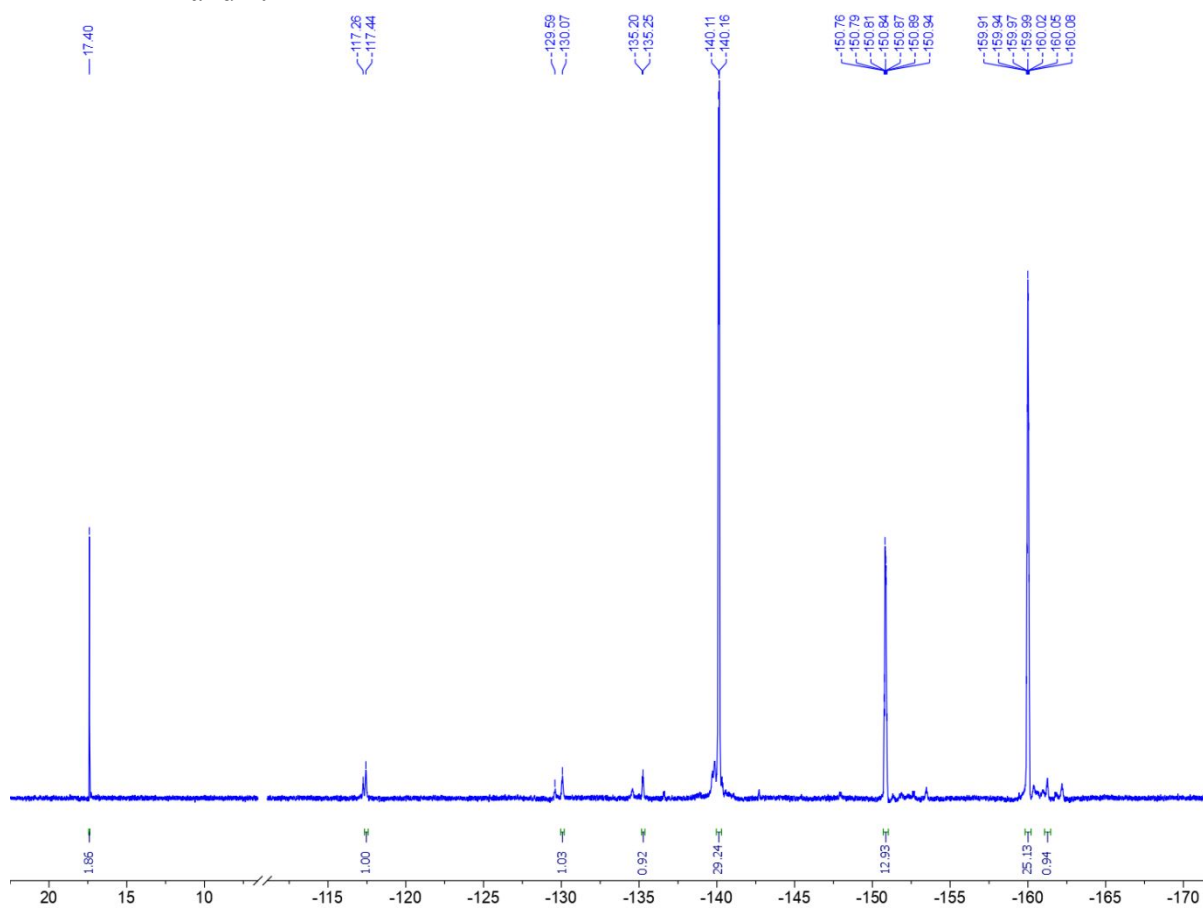
2.1 Figure S1. ^1H NMR spectrum of **2**.



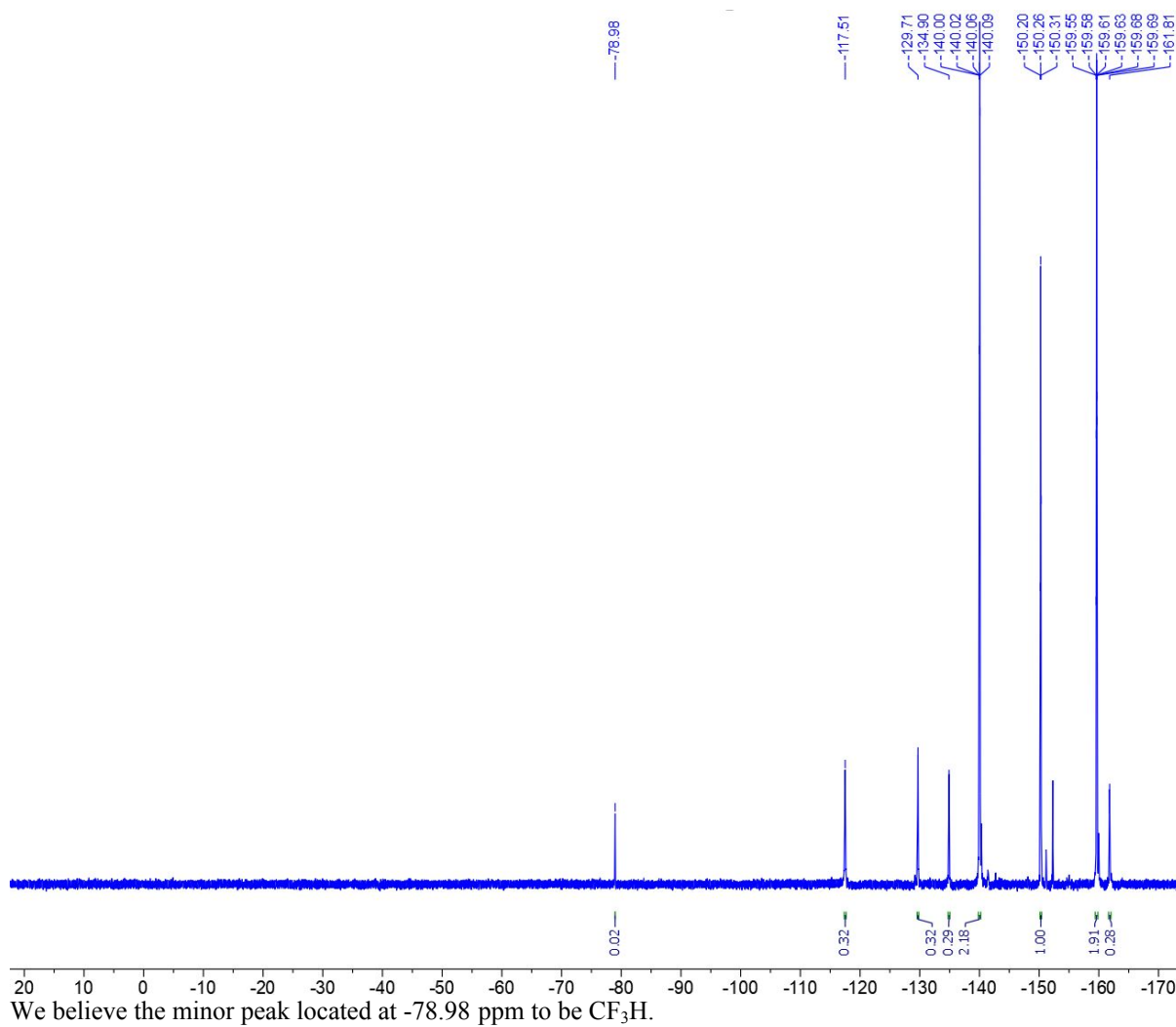
2.2 Figure S2. ^{19}F NMR spectrum of **2**.



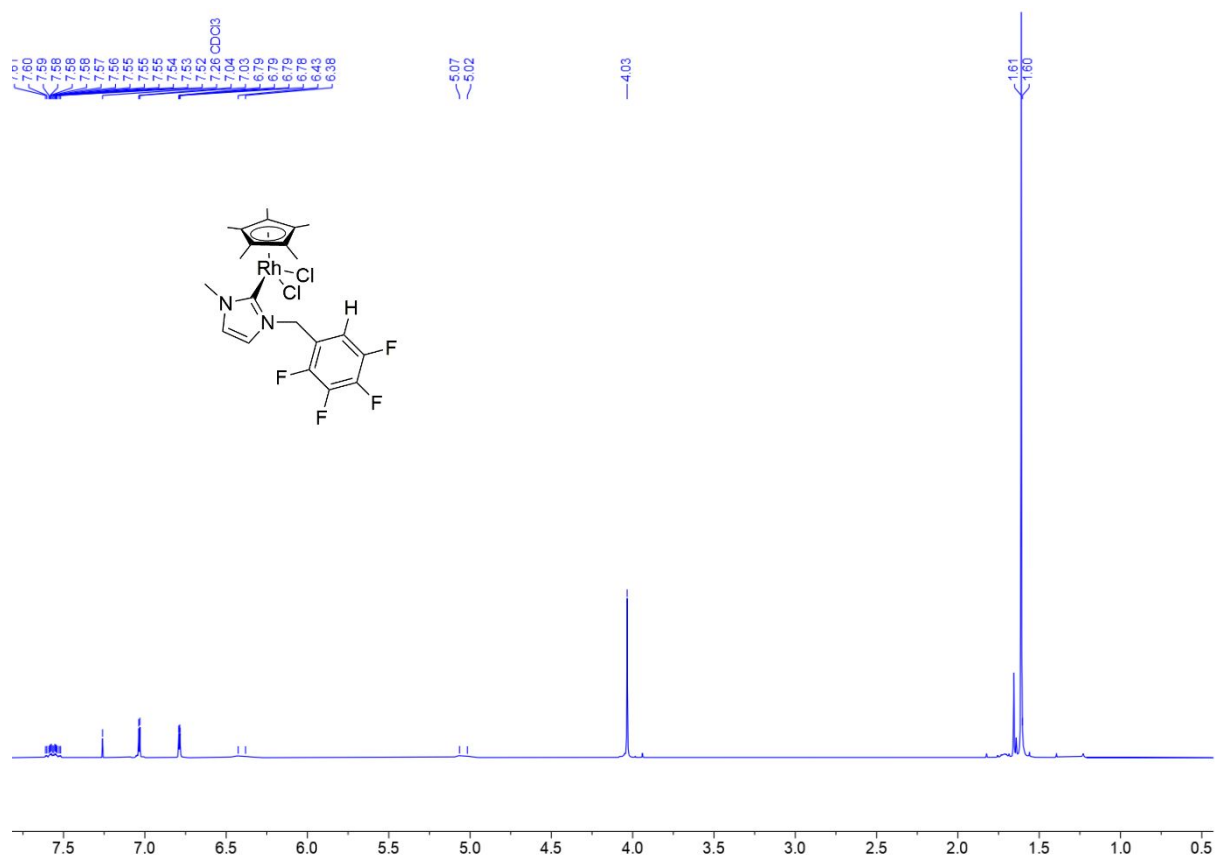
2.3 **Figure S3.** ^{19}F NMR spectrum of reaction mixture with toluoyl fluoride and **2**.



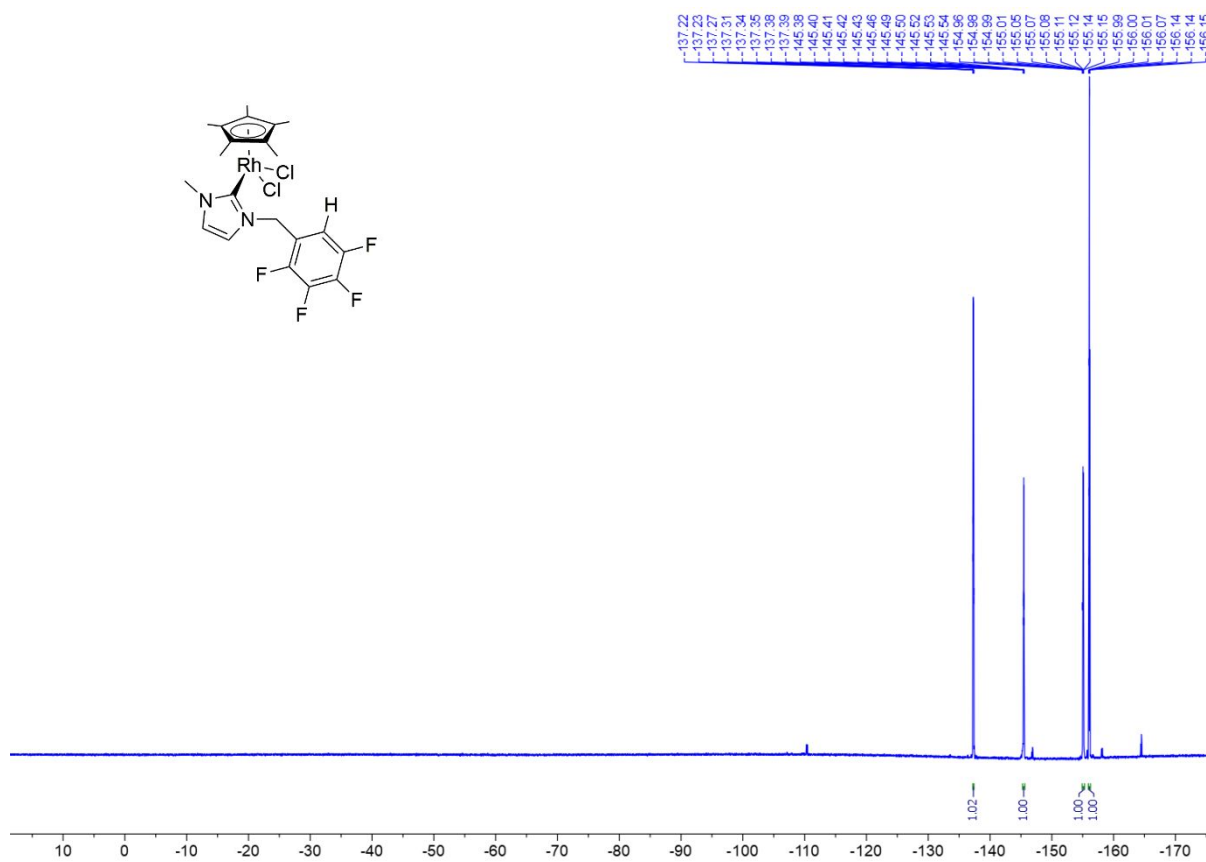
2.4 Figure S4. ^{19}F NMR spectrum of $\text{RhCp}^*\text{Cl}_2(\text{F}_5\text{Bzmim})$ and **2** showing conversion.



2.5 Figure S5. ^1H NMR spectrum of $[\text{Cp}^*\text{RhCl}_2(\kappa\text{C-MeNC}_3\text{H}_2\text{NCH}_2\text{C}_6\text{HF}_4)]$.

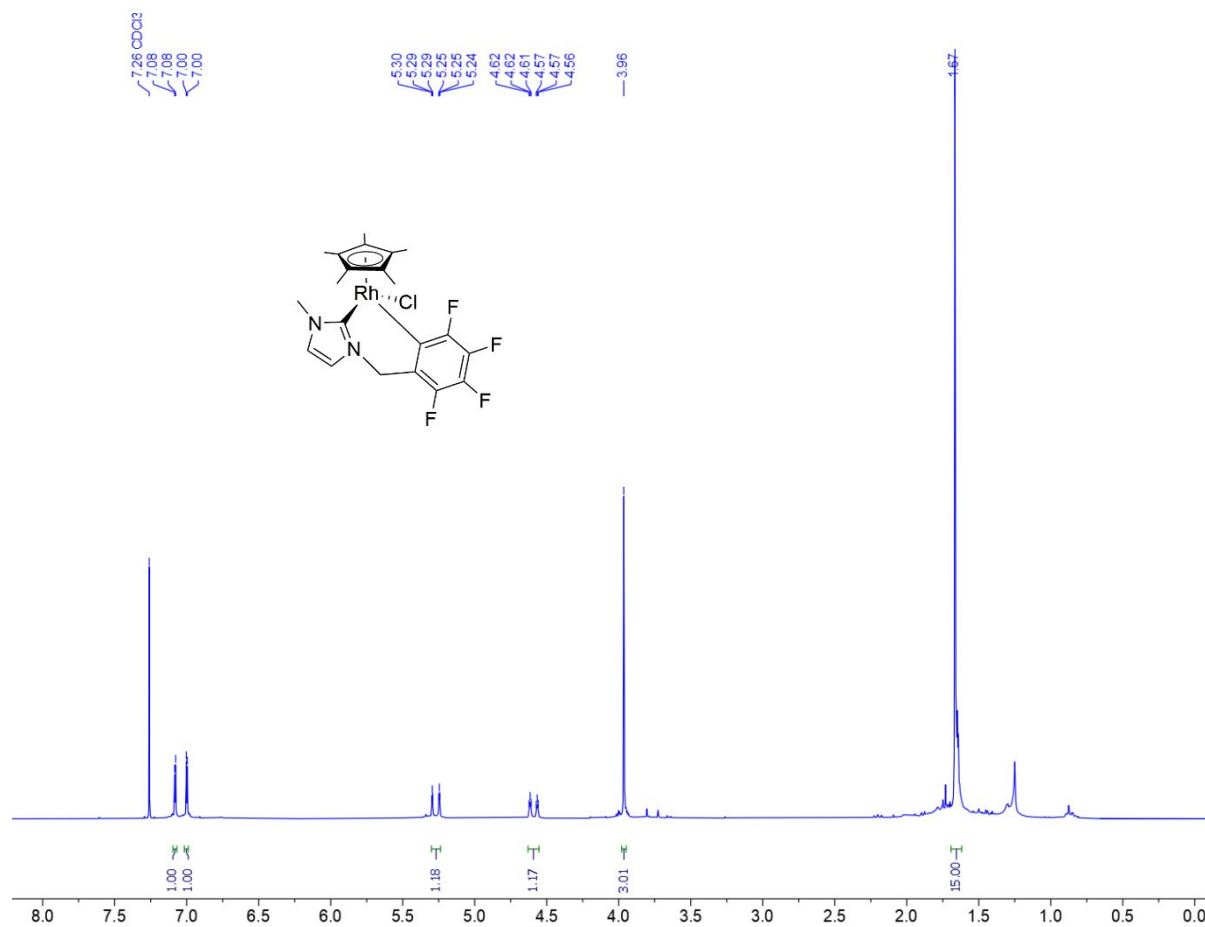


2.6 Figure S6. ^{19}F NMR spectrum of $[\text{Cp}^*\text{RhCl}_2(\kappa\text{C-MeNC}_3\text{H}_2\text{NCH}_2\text{C}_6\text{HF}_4)]$.

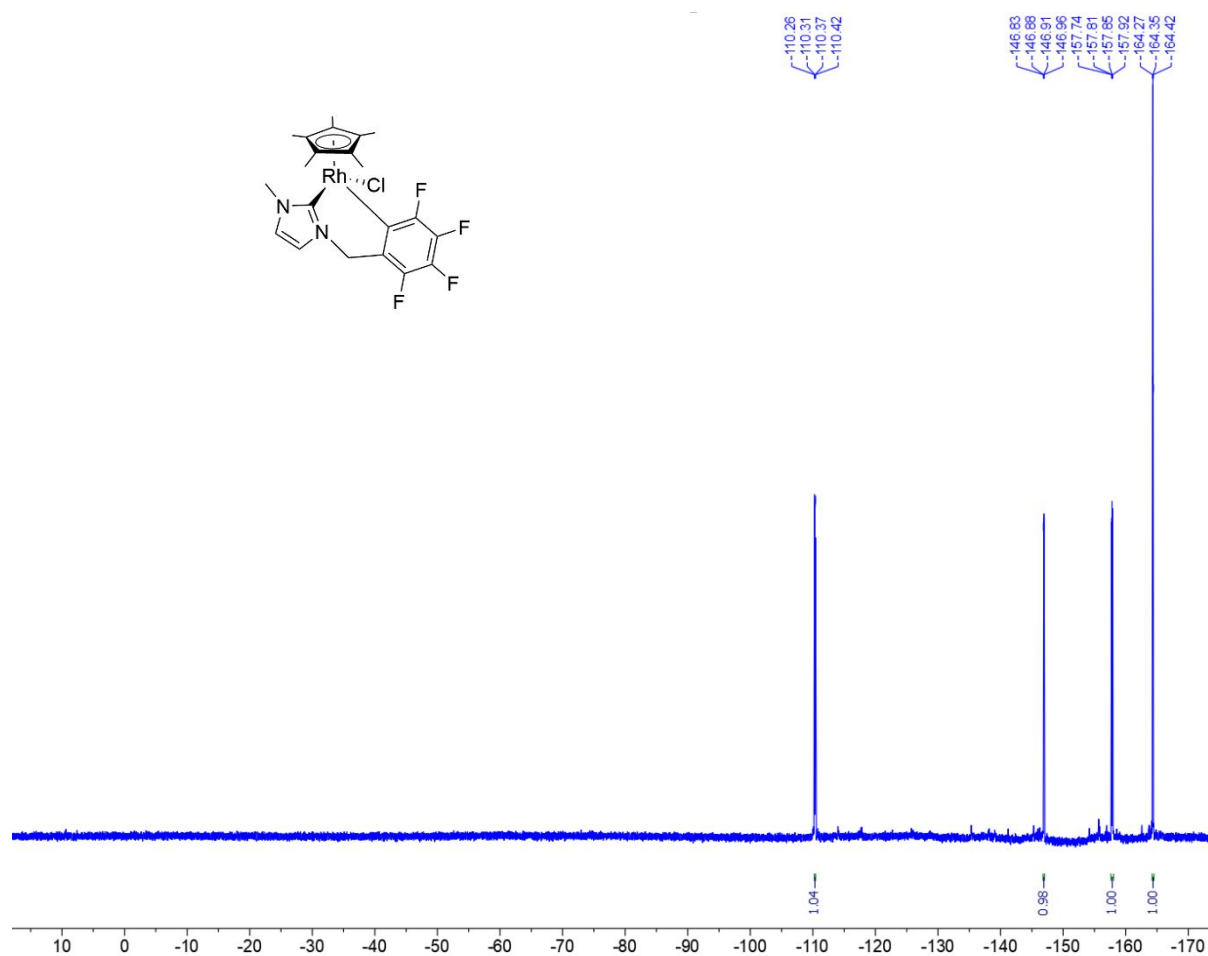


Contains $[\text{Cp}^*\text{RhCl}_2(\kappa\text{C-MeNC}_3\text{H}_2\text{NCH}_2\text{C}_6\text{HF}_4)]$ and 4 minor peaks of **3**.

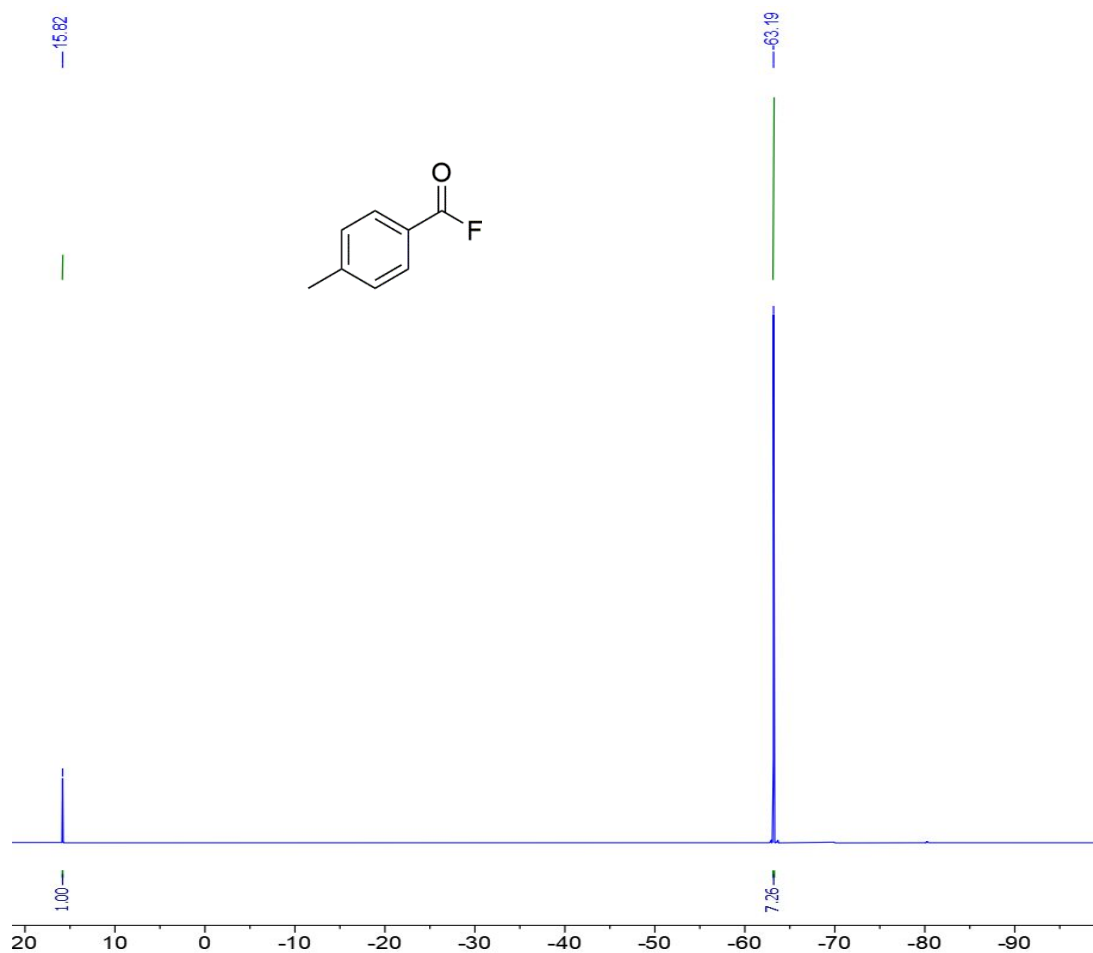
2.7 Figure S7. ^1H NMR spectrum of $[\text{Cp}^*\text{RhCl}(\kappa\text{C}^2\text{-MeNC}_3\text{H}_2\text{NCH}_2\text{C}_6\text{F}_4)]$, **3**.



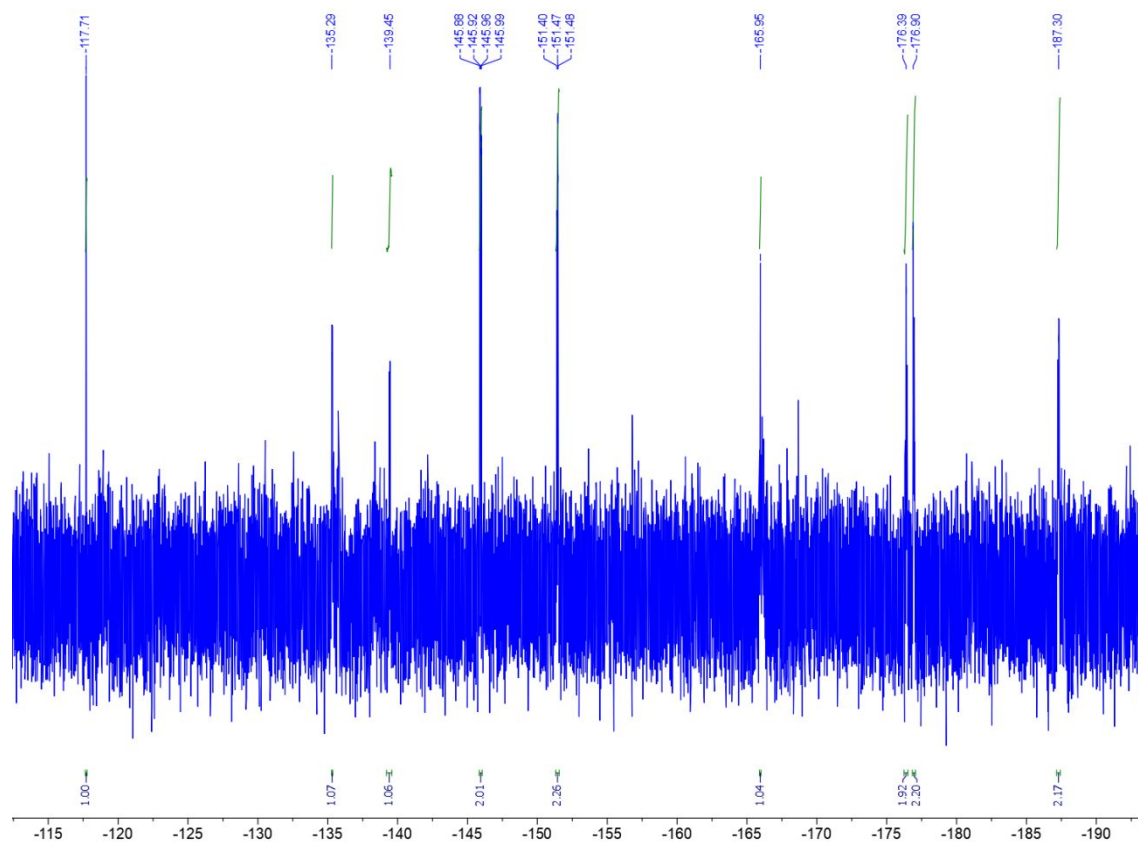
2.8 Figure S8. ^{19}F NMR spectrum of $[\text{Cp}^*\text{RhCl}(\kappa\text{C}^2\text{-MeNC}_3\text{H}_2\text{NCH}_2\text{C}_6\text{F}_4)]$, **3**.



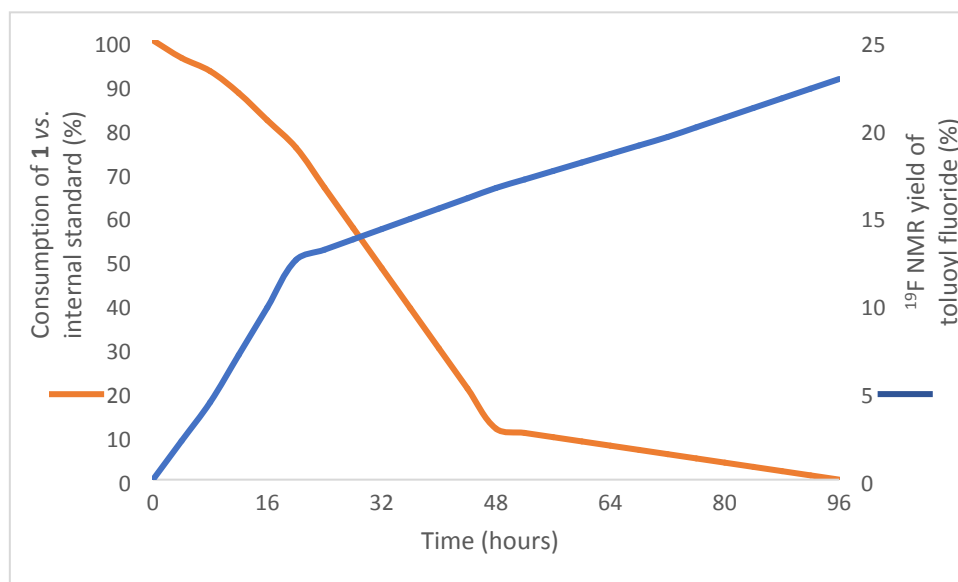
2.9 Figure S9. ^{19}F NMR spectrum of toluoyl fluoride following UV photolysis, with internal standard.



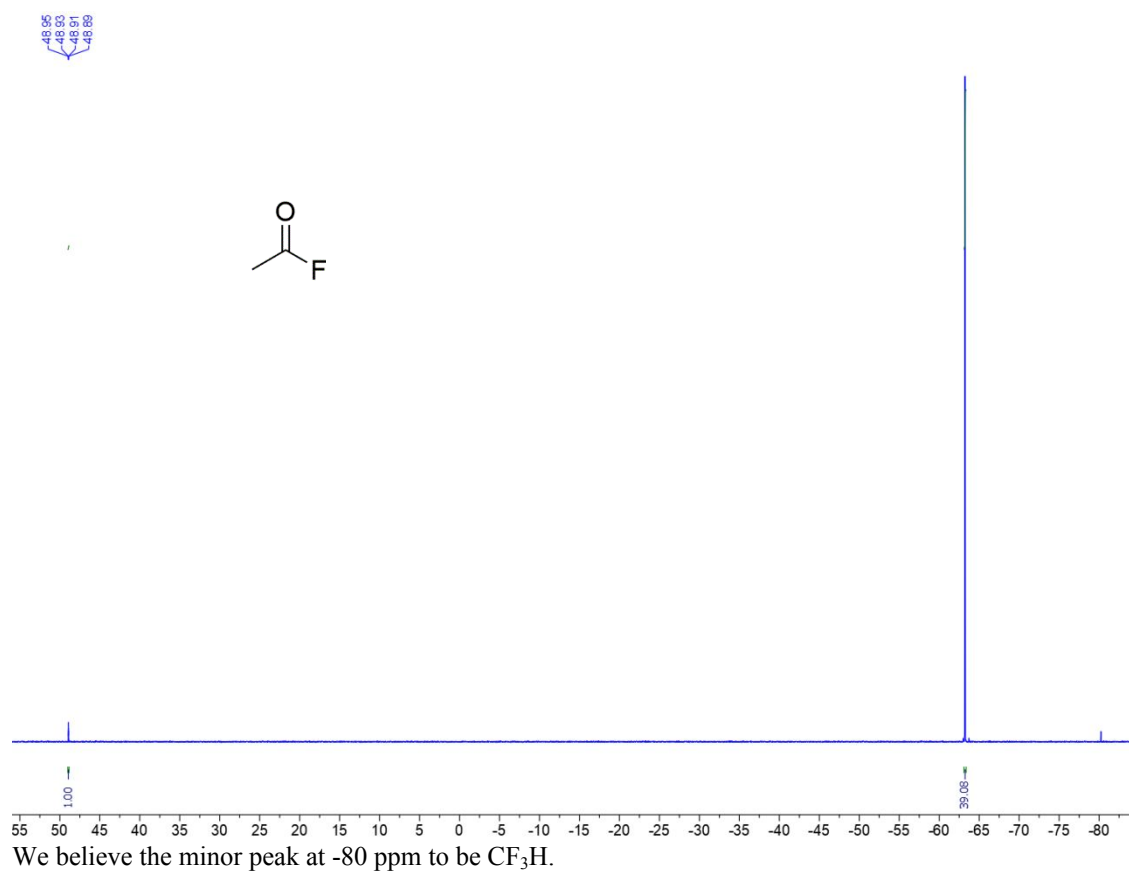
2.10 Figure S10. ^{19}F NMR spectrum of sediment from walls of cuvette following UV photolysis. Contains a mixture of **1** and **2**.



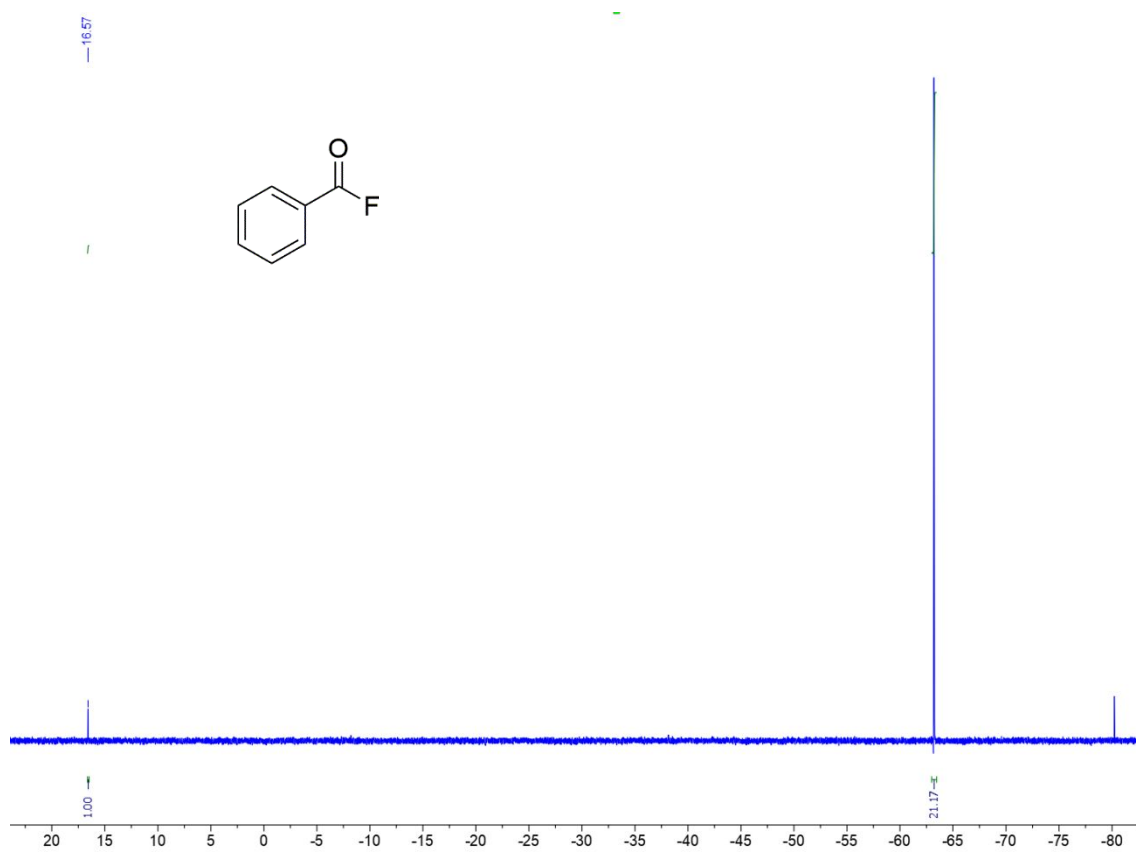
2.11 Figure S11. Plot showing rate of formation of toluoyl fluoride and consumption of **1** over 96 hours, monitored over time with ^{19}F NMR.



2.12 Figure S12. ^{19}F NMR spectrum of acetyl fluoride.

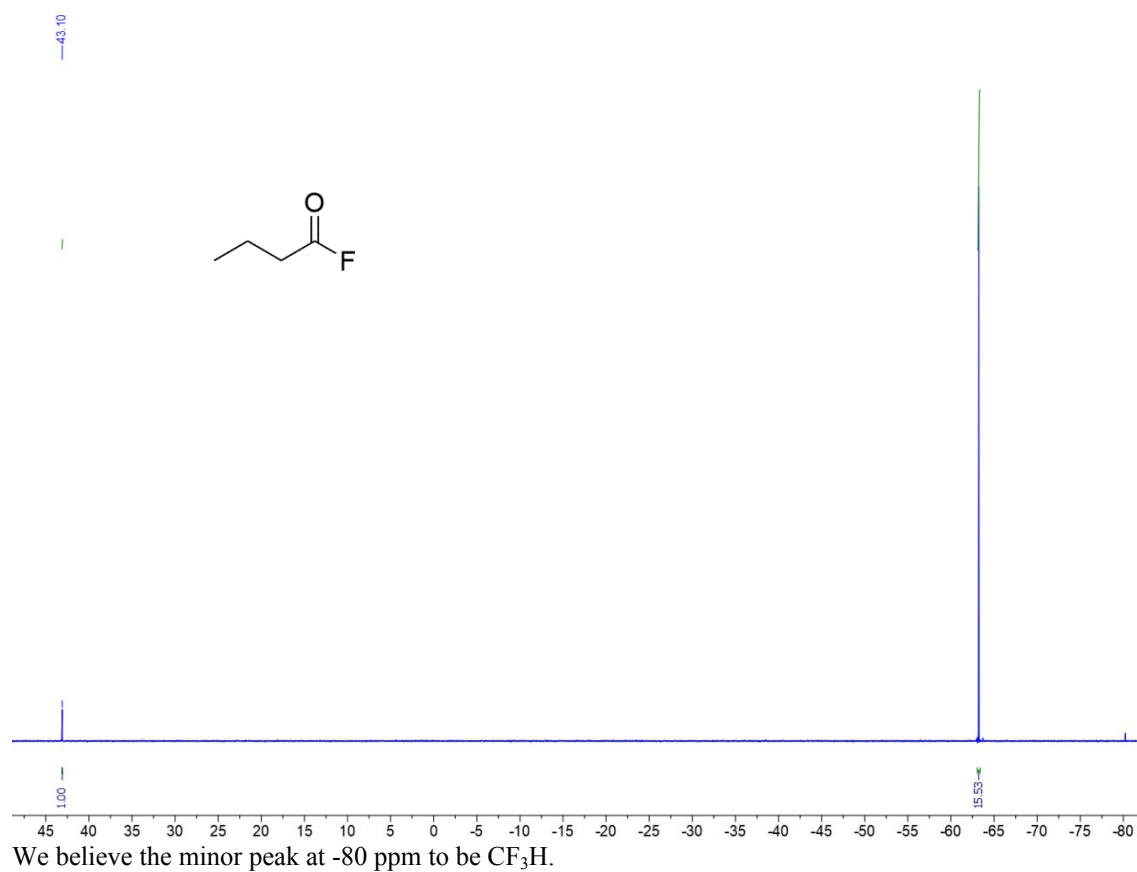


2.13 Figure S13. ^{19}F NMR spectrum of benzoyl fluoride.

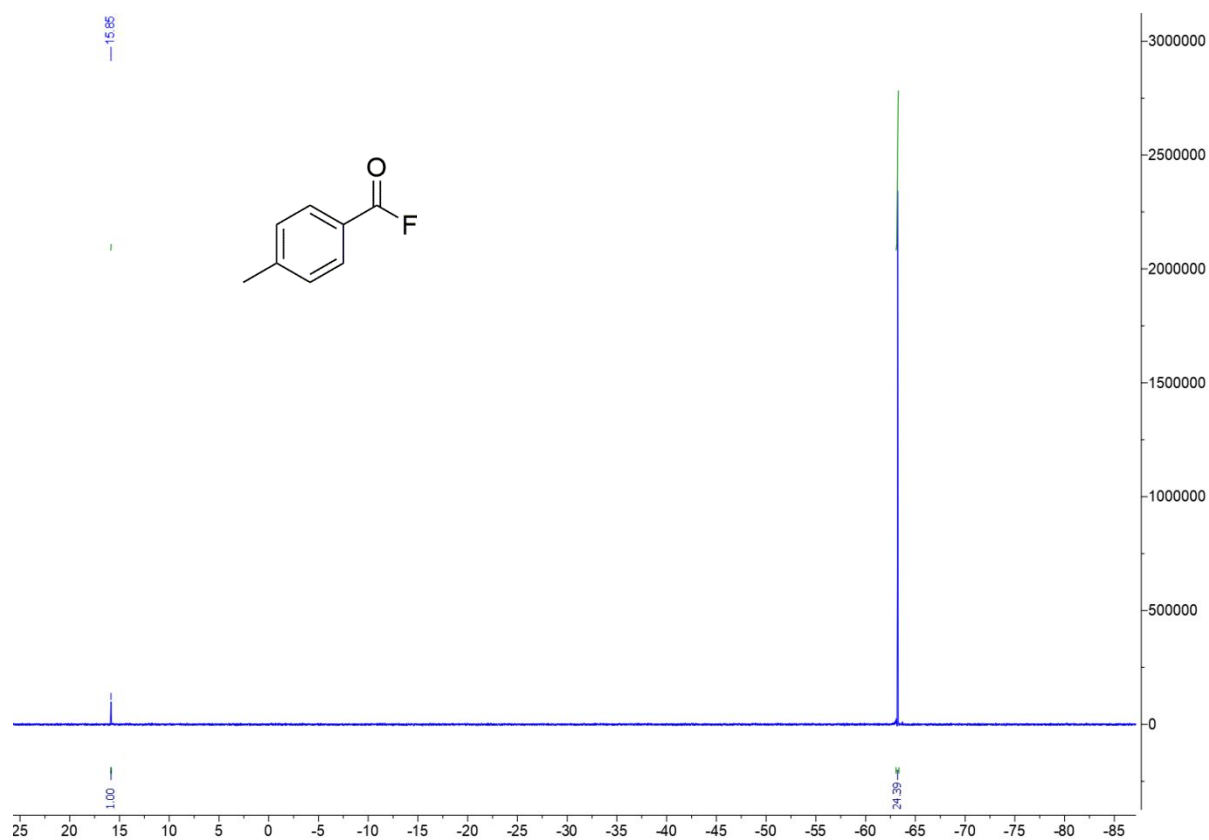


We believe the minor peak at -80 ppm to be CF_3H .

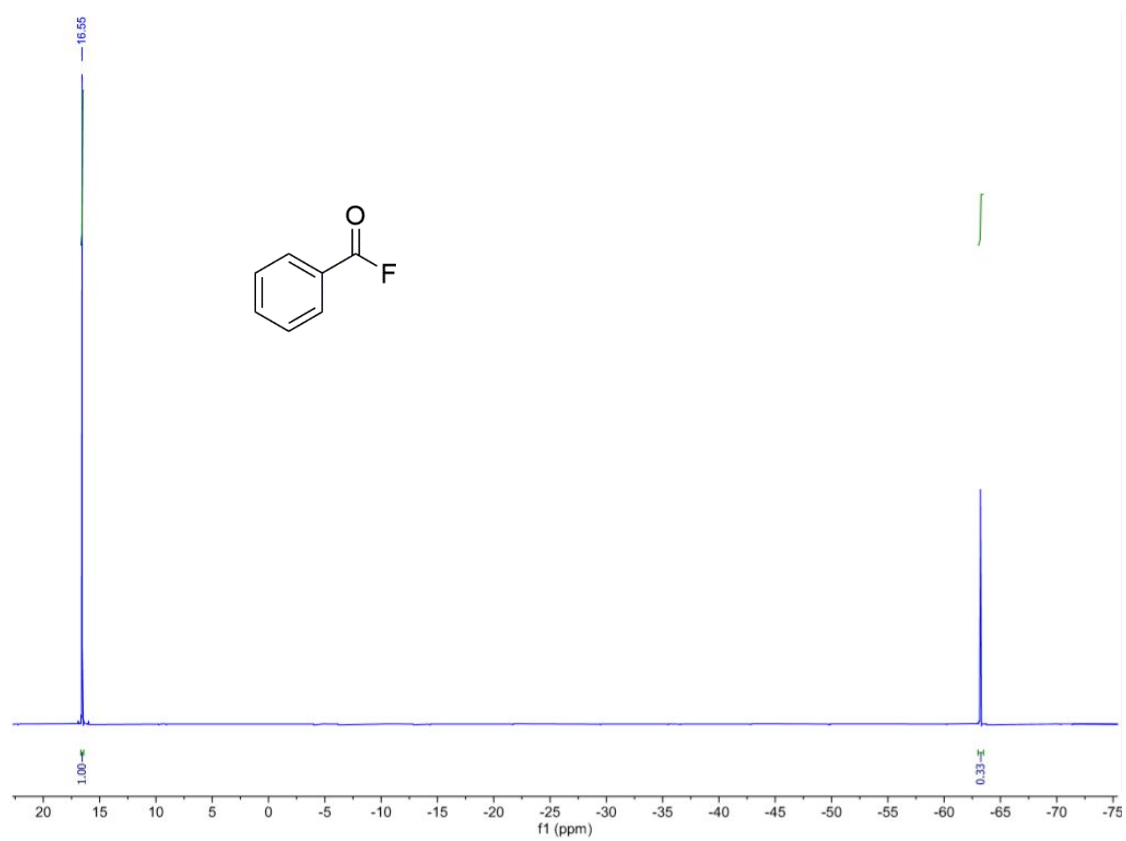
2.14 Figure S14. ^{19}F NMR spectrum of butyryl fluoride.



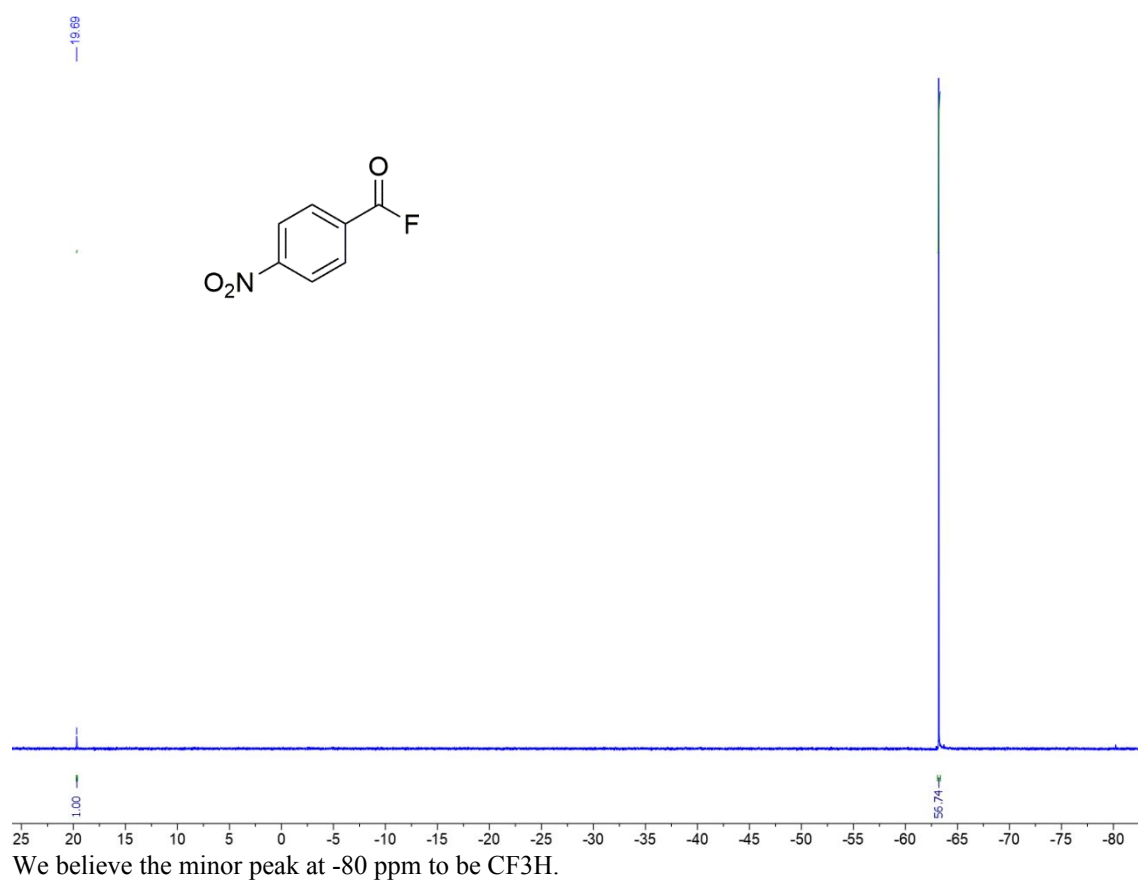
2.15 Figure S15. ^{19}F NMR spectrum of toluoyl fluoride.



2.16 Figure S16. ^{19}F NMR spectrum of benzoyl fluoride.

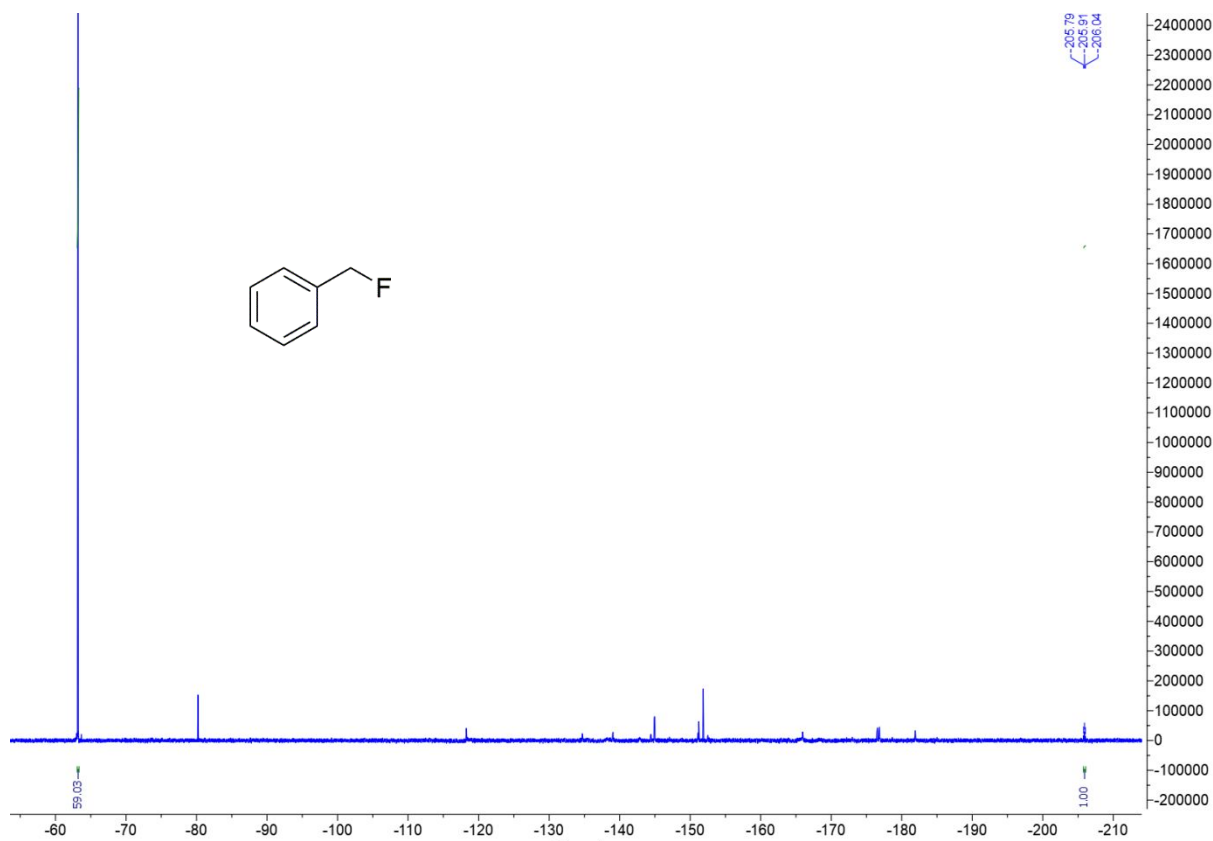


2.17 Figure S17. ^{19}F NMR spectrum of 4-nitrobenzoyl fluoride.



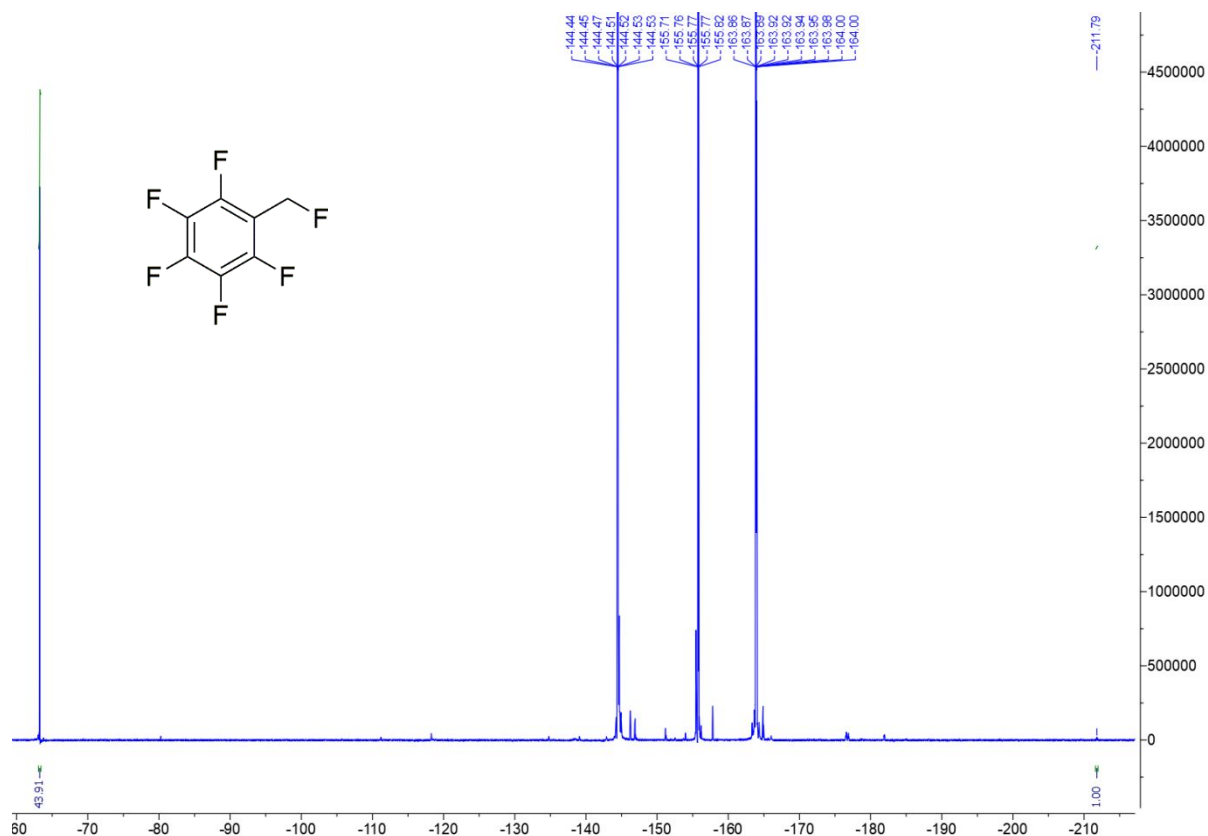
We believe the minor peak at -80 ppm to be CF_3H .

2.18 Figure S18. ^{19}F NMR spectrum of benzyl fluoride.



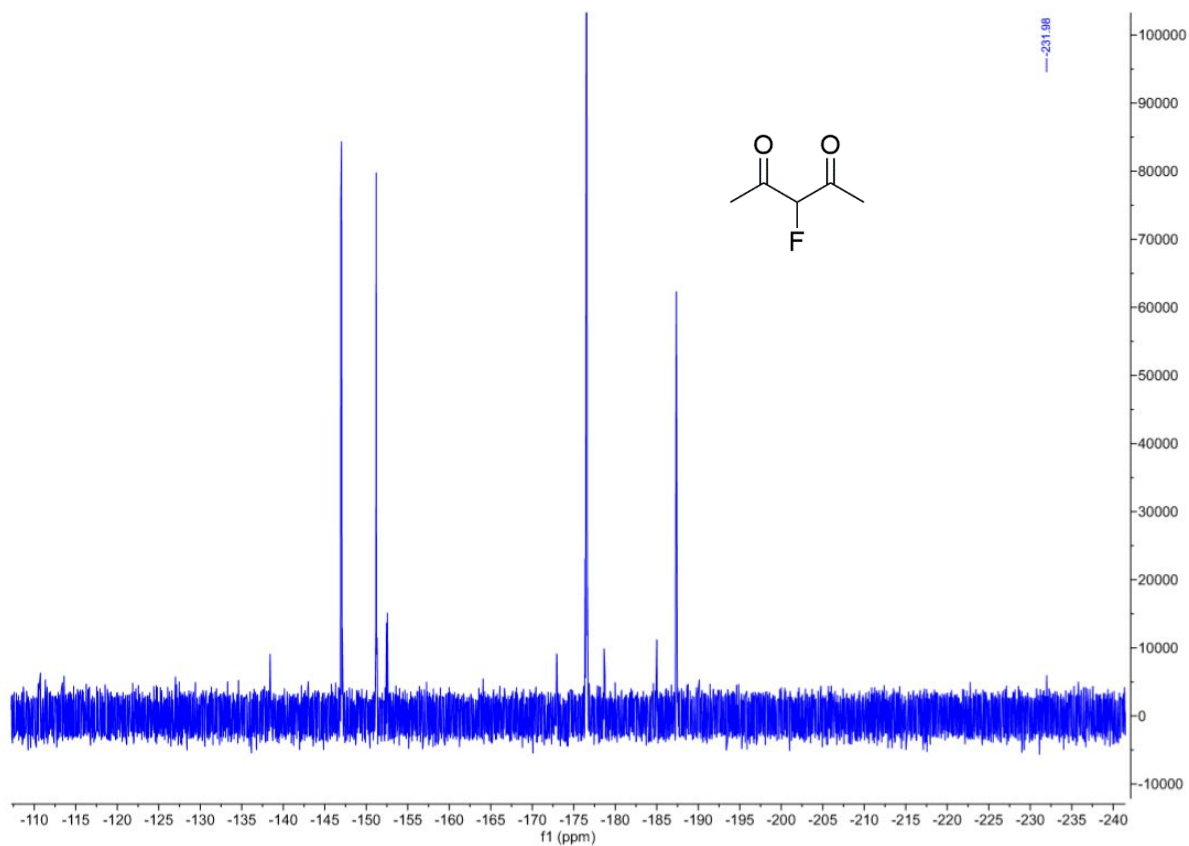
A number of additional peak are present in the spectra. In addition to the internal standard (trifluorotoluene) (-63.72 ppm) and benzyl fluoride (-205.91 ppm), the peaks present are a mixture of **1**, **2** and $\text{RhCp}^*\text{Cl}_2(\text{F}_5\text{Bmim})$. We believe the minor peak at -80 ppm to be CF_3H .

2.19 Figure S19. ^{19}F NMR spectrum of 2,3,4,5,6-pentafluorobenzyl fluoride.



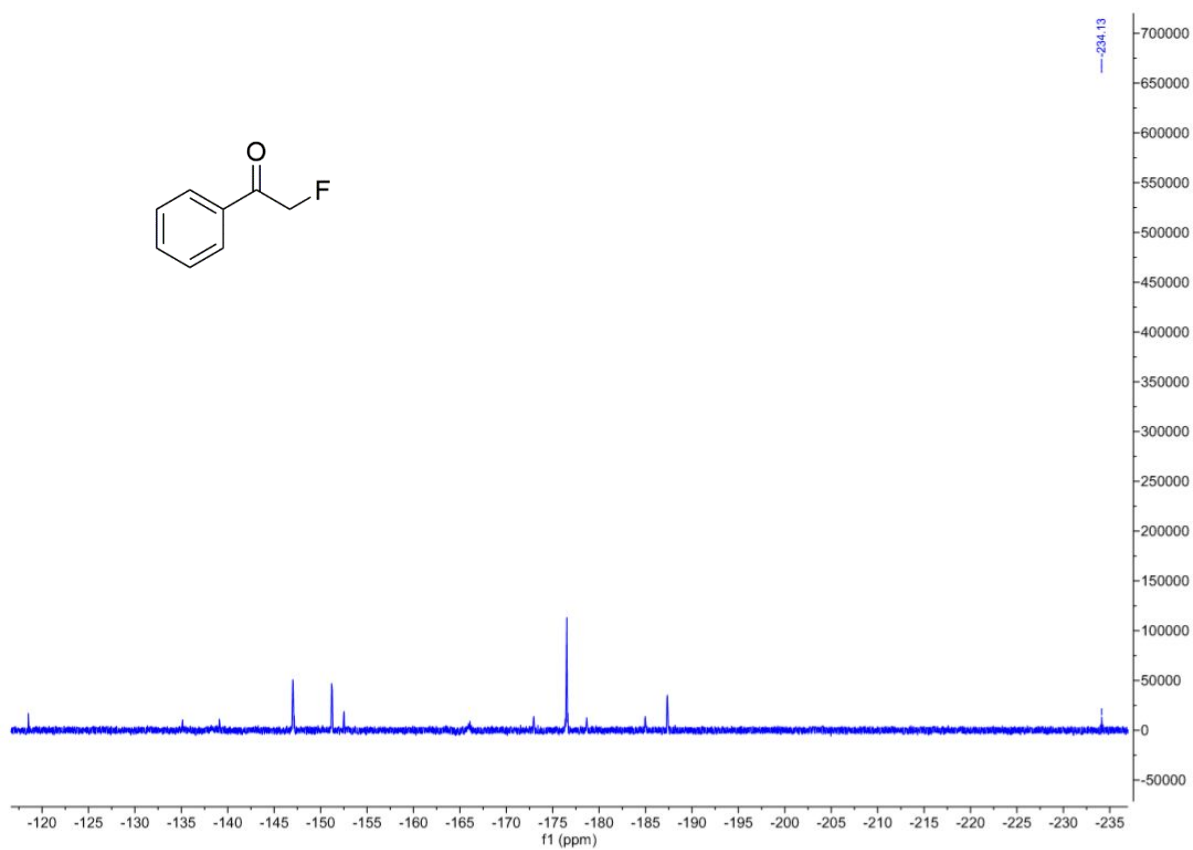
A number of additional peak are present in the spectra. In addition to the internal standard (trifluorotoluene) (-63.72 ppm) and 2,3,4,5,6-pentafluorobenzyl fluoride (-211.79 ppm), the peaks present are a mixture of **1** and **2**. We believe the minor peak at -80 ppm to be CF_3H .

2.20 Figure S20. ^{19}F NMR spectrum of 3-fluoropenta-2,4-dione.



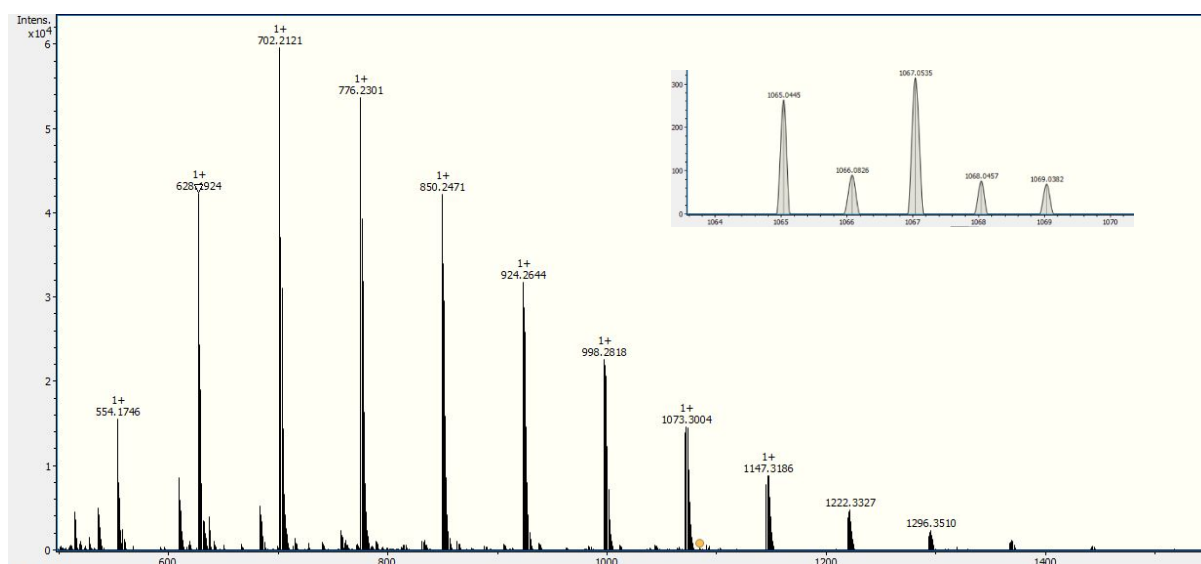
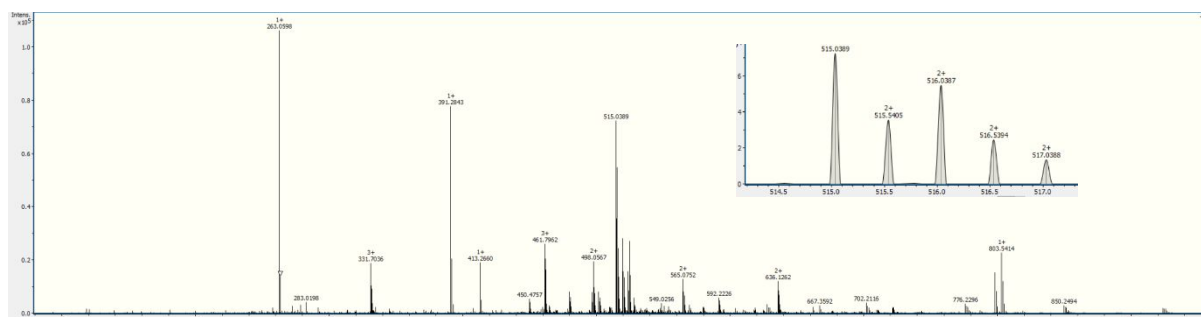
In addition to 3-fluoropenta-2,4-dione (-231.98 ppm), the peaks present are a mixture of **1** and **2**.

2.21 Figure S21. ^{19}F NMR spectrum of 2-fluoroacetaphenone.

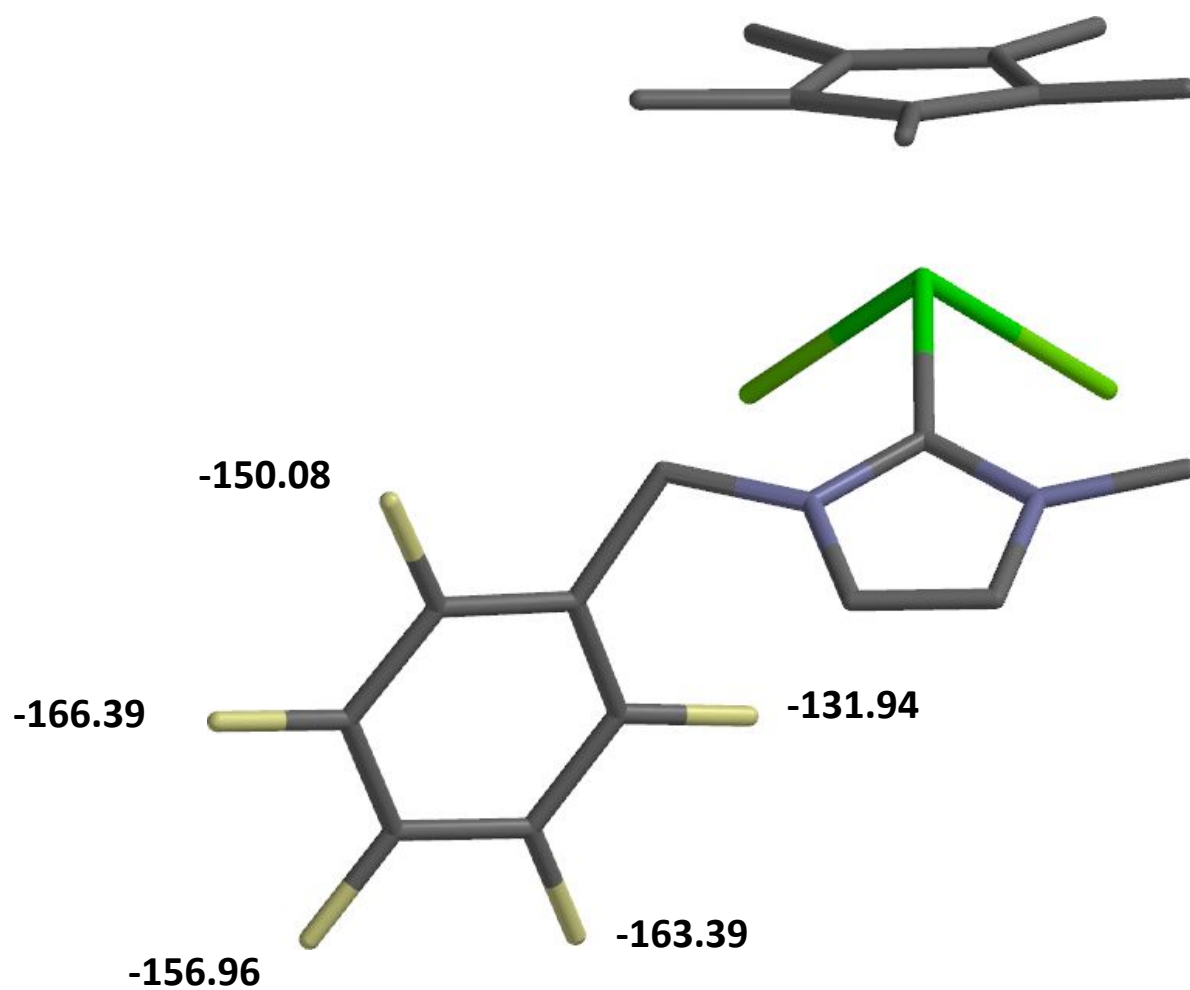


In addition to 2-fluoroacetaphenone (-234.13 ppm), the peaks present are a mixture of **1** and **2**.

2.22 Figure S22. Electrospray mass spectrum of **2**.



2.23 Figure S23. Calculated ^{19}F NMR chemical shift of $\text{RhCp}^*\text{Cl}_2(\text{F}_5\text{Bzmim})$.



2.24 Figure S24. Calculated ^{19}F NMR chemical shift of **1**.

